On non-stationary response of cracked thin rectangular plates acted upon by a moving random force

Ali Nikkhoo*[a]· Shirin Banihashemi [a]· Keivan Kiani [b]

a. Department of Civil Engineering University of Science and Culture (USC), Tehran, Iran
b. Department of Civil Engineering, K. N. Toosi University of Technology, Tehran, Iran

Abstract

This paper is aimed to examine the dynamics of cracked thin rectangular plates subjected to a moving non-stationary random load. A random load is considered with a constant mean value, a constant moving velocity, and five different covariance patterns namely the white noise, constant, exponential, cosine wave, and exponential cosine covariance. Accordingly, an intact plate's orthogonal polynomials in combination with the well-known corner functions are employed to explore the mechanical behavior of the cracked plate. As the non-dimensional deflection values, the functions of the squared mean values are obtained for the damped and undamped cracked plates at different points. Then an inclusive parametric study is performed to explore effects of the inclined crack angles and the crack lengths on the non-dimensional functions of squared mean values at middle point of the undamped and damped cracked plates. Based on the obtained results, there are non-monotonous nonlinear relations between increasing the incline crack angles as well as the crack lengths and the non-dimensional functions of squared mean values. Furthermore, it is found that in the exponential covariance cases, the effects of increasing crack angles and lengths on the non-dimensional squared mean values are profounder than the other four patterned covariance cases.

Keywords Cracked thin plate · Dynamic vibration · Moving non-stationary random load · Orthogonal polynomials · Corner functions · Squared mean value

1. Introduction

The engineering structures are subjected to unknown moving loads during their lifecycle, obeyed the random processes or the random functions of time or location. The random vibration in mechanical systems was developed by Crandall [1]. Through 1965 and 1967, the introduction to non-stationary random processes was presented by Priestley [2, 3]. As many structures such as transport structures, are subjected to a kind of moving random load, in 1976, a beam subjected to a moving non-stationary random load with a constant velocity and a mean value was investigated by Fryba [4]. After that, the dynamic vibration of a beam subjected to a series of random moving loads with random velocities, was proposed by Sniady [5]. In another research project, dynamic vibrations of a beam subjected to a series of random moving loads with a constant velocity, were studied by Sieniawska and Sniady [6]. Moreover, the responses of a beam subjected to a moving load with a random velocity were studied by Sniady et al. [7]. Rystwej and Sniady [8] investigated the vibrations of an infinite beam and a plate, sitting on a Pasternak foundation, subjected to a crossing moving random load with a constant velocity. Malara and Spanos [9] managed to evaluate the nonlinear responses of a plate due to the vibrations induced by the random loads. Sniady et al. [10] studied the behavior of the Euler-Bernoulli beam, subjected to the Gaussian white noise as a random vibration. Kong and Spanoc [11], evaluated the nonlinear vibration of a plate, subjected to the Brownian noise or red noise. Furthermore, the vibration of a rectangular-shaped system subjected to the white noise was studied by Jiao and Spanos [12]. Spanos and Malara [13] studied the nonlinear vibration of the simply-supported beams and plates subjected to the Brownian noise. A linearization of a nonlinear single degree of freedom system subjected to the deterministic and the White noise as a random load was presented by Zhang and Spanos [14].

*. Corresponding author. Tel: +98 21 44252045;
P. O. Box 13145-871, Tehran, Iran;
E-mail: nikkhoo@usc.ac.ir (Ali Nikkhoo)

The vibration of nonlinear elastic impact oscillator with Coulomb friction subjected to the White noise was studied by Liu et. al. [15]. Thereafter, a two-degree-of-freedom system subjected to the random excitation was analyzed by Podworna et al. [16] as a model of the transport structure and the structure vibration absorber. Jablonka and Iwankiewicz [17] investigated the vibrations of a beam subjected to the moving random loads. The vibration of a beam form structure subjected to moving random loads was investigated by Golcki et al. [18].

According to the researchers' reports [19 – 26], moving masses, whose inertial effects are considered, have impact on plates' deflections. Rofooei and Nikkhoo [19] revealed the moving mass effect on a plate displacement, especially for larger mass weights and/or larger velocities. In another study, Nikkhoo and Rofooei [20] examined the importance of the inertial effect, by using all acceleration terms of the moving mass. Nikkhoo et al. [21], investigated the excitation of a thin rectangular plate subjected to series of moving masses. Ghazvini et al. [22] studied the dynamic vibration of thin un-uniform profile rectangular plates under the force of a moving mass. Hassanabadi et al. [23] investigated the resonance of thin rectangular plates subjected to a train of moving mass. Rofooei et al. [24] collated the Von Karman and Kirchhoff plate theory to explore the deflection of rectangular plates subjected to a moving mass. In another research attempt, Nikkhoo et al. [25], explored the excitations of flexo – poro elastic structures resting on the elastic foundations subjected to the moving loads. In another study, Nikkhoo et al. [26], evaluated effects of the moving mass' weights, velocities, plates' aspect ratios, inclined crack angles, and crack lengths.

In the present study, for the first time, the vibration of a rectangular thin plate with a surface constant crack subjected to a moving non-stationary random load with a constant velocity and a constant mean value is investigated for five various covariance patterns, namely the white noise, constant, exponential, cosine wave and the exponential cosine covariance. The non-dimensional deflection values at different points of the undamped and damped cracked plates are obtained. To this end the intact plate orthogonal polynomials in combination with the well-known corner functions are employed to define the behavior of the cracked plate. Further, a parametric investigation is performed to determine the effects of the inclined crack angles and the crack lengths on the non-dimensional deflection values at the middle point of the undamped and damped cracked plates as well.

2. Problem Definition

The partial differential equation of motion of a uniform thin rectangular plate, subjected to a moving load, is expressed as follows [27]:

$$D\nabla^4 W(x,y,t) + c\frac{\partial W(x,y,t)}{\partial t} + m\frac{\partial^2 W(x,y,t)}{\partial t^2} = P(x,y,t) = \delta(x-x_0)\delta(y-y_0)P(t) \tag{1}$$

where $W(x, y, t)$ is the vertical deflection of the plate at any time-dependent coordinates x, y.

$D = \dfrac{Eh^3}{12(1-\nu^2)}$, is the plate's flexural rigidity, where E, ν, and h are the plate's modulus of elasticity, Poisson's ratio and thickness, respectively. Accordingly, m, and c are the mass per unit area and damping constant of the plate respectively. The free vibration response of the plate is assumed as:

$$W(x,y,t) = \sum_{i=1}^{\infty}\sum_{j=1}^{\infty}\phi_{ij}(x,y)e^{\bar{\imath}\,\omega_{ij}t} \tag{2}$$

where $\phi_{ij}(x, y)$, ω_{ij}, and $\bar{\imath}$ are the ijth vibration mode, the natural frequency of the plate and the imaginary unit, respectively. It is assumed that the mode shape of the plate, $\phi_{ij}(x, y)$, is taken into account. Moreover, it is assumed that the random process is sum of random variables, whose probability distribution is determinate by time, and a zero mean random process, that are revealed in the equation (5) respectively [4, 28]:

$$P(x,y,t) = \begin{cases} P(x,y,t) & t \geq 0 \\ 0 & t < 0 \end{cases} \tag{3}$$

$$P(x,y,t) = \delta(x-x_0)\delta(y-y_0)P(t) \qquad x_0 = vt\ ,\ y_0 = b/2 \tag{4}$$

$$P(t) = P + P_0(t) \quad , \quad E[P(t)] = P \tag{5}$$

where the *E* operator, and *v* are the linear function of the mean value and the constant velocity of the moving load respectively.

R_{pp}, the covariance is achieved as following equations:

$$R_{pp}(t_1,t_2)=E[P_0(t_1)P_0(t_2)] \tag{6}$$

$$E[P(x,y,t)]=\delta(x-x_0)\delta(y-y_0)P \tag{7}$$

$$P_0(x,y,t)=\delta(x-x_0)\delta(y-y_0)P_0(t) \tag{8}$$

$$R_{pp}(x_1,y_1,x_2,y_2,t_1,t_2)=E[\delta(x_1-vt_1)\delta(y_1-y_0)P_0(t_1)\delta(x_2-vt_2)\delta(y_2-y_0)P_0(t_2)] \tag{9}$$

$$R_{pp}(x_1,y_1,x_2,y_2,t_1,t_2)=\delta(x_1-vt_1)\delta(y_1-y_0)\delta(x_2-vt_2)\delta(y_2-y_0)R_{pp}(t_1,t_2) \tag{10}$$

The covariance of the generalized moving random load is:

$$R_{Q_{ij}Q_{kl}}(t_1,t_2)=\int_{-\infty}^{\infty}\int_{-\infty}^{\infty}\int_{-\infty}^{\infty}\phi_{ij}(x_1,y_1)\phi_{kl}(x_2,y_2)\delta(x_1-vt_1)\delta(y_1-y_0)\delta(x_2-vt_2)\delta(y_2-y_0)R_{pp}(t_1,t_2)dx_1dx_2dy_1dy_2=\phi_{ij}(vt_1,y_0)\phi_{kl}(vt_2,y_0)R_{pp}(t_1,t_2) \tag{11}$$

The covariance of the generalized deflection is:

$$R_{w_{ij}w_{kl}}(t_1,t_2)=\int_{-\infty}^{\infty}\int_{-\infty}^{\infty}h_{ij}(t_1-\tau_1)h_{kl}(t_2-\tau_2)\phi_{ij}(v\tau_1,y_0)\phi_{kl}(v\tau_2,y_0)R_{pp}(t_1,t_2)d\tau_1d\tau_2 \tag{12}$$

$$R_{w_{ij}w_{kl}}(t_1,t_2)=\int_{-\infty}^{\infty}\int_{-\infty}^{\infty}h_{ij}(\tau_1)h_{kl}(\tau_2)\phi_{ij}(v\tau_1-vt_1,y_0)\phi_{kl}(v\tau_2-vt_2,y_0)R_{pp}(\tau_1-t_1,\tau_2-t_2)d\tau_1d\tau_2 \tag{13}$$

$$R_{w_{ij}w_{kl}}(x_1,y_1,x_2,y_2,t_1,t_2)=\sum_{i=1}^{n}\sum_{j=1}^{n}\sum_{k=1}^{n}\sum_{l=1}^{n}\phi_{ij}(x_1,y_1)\phi_{kl}(x_2,y_2)\phi_{ij}(x_0,y_0)\phi_{kl}(x_0,y_0)\int_{-\infty}^{\infty}\int_{-\infty}^{\infty}h_{ij}(\tau_1)h_{kl}(\tau_2)\phi_{ij}(v\tau_1-vt_1,y_0)\phi_{kl}(v\tau_2-vt_2,y_0)R_{pp}(t_1-\tau_1,t_2-\tau_2)d\tau_1d\tau_2 \tag{14}$$

$$E\left[w^2(x,y,t)\right]=R_{Q_{ij}Q_{kl}}(x,x,y,y,t,t) \tag{15}$$

$$E\left[w^2(x,y,t)\right]=\sum_{i=1}^{n}\sum_{j=1}^{n}\sum_{k=1}^{n}\sum_{l=1}^{n}\phi_{ij}(x,y)\phi_{kl}(x,y)\phi_{ij}(x_0,y_0)\phi_{kl}(x_0,y_0)\int_0^t\int_0^t h_{ij}(\tau_1)h_{kl}(\tau_2)\phi_{ij}(vt-v\tau_1,y)\phi_{kl}(vt-v\tau_2,y)R_{pp}(t-\tau_1,t-\tau_2)d\tau_1d\tau_2 \tag{16}$$

where the *h* operator is the impulse function:

$$h_{ij}(\tau)=\{0 \quad for\ \tau<0 \quad , \quad \frac{1}{\omega_{ij}'}e^{-\omega_b\tau}\sin(\omega_{ij}'\tau) \quad for\ \tau\geq 0 \tag{17}$$

$$\omega_{ij}'^2=\omega_{ij}^2-\omega_b^2 \tag{18}$$

in which ω_{ij}', ω_{ij}, and ω_b are the natural frequency of the damped plate, the natural frequency of the undamped plate and the damping coefficient respectively. For most structures, the damping coefficient is below 20% of the natural frequency of the undamped plate. In present investigation, the damping coefficient is designated below 10% of the natural frequency of the undamped plate.

The mode shapes of a simply-supported rectangular intact plate are as follows and the mode shapes of other boundary conditions also can be considered as given below [29]:

$$\phi_{ij}(x,y) = 2\sin(\frac{i\pi x}{a})\sin(\frac{j\pi y}{b}) \tag{19}$$

Five types of the covariance of the force $P(t)$, the white noise, constant covariance, exponential cosine, exponential and the cosine wave, are taken into account.

For the white noise, the covariance and the spectral density are determined as follows:

$$R_{pp}(\tau_1,\tau_2) = 2\pi S_p \delta(\tau_2 - \tau_1) \quad , \quad S_{pp}(\omega_1,\omega_2) = S_p \tag{20}$$

where S_p is the constant spectral density and δ is Dirac delta function.

The squared mean value is obtained as follows:

$$E[w^2(x,y,t)] = 2\pi S_p \sum_{i=1}^{n}\sum_{j=1}^{n}\sum_{k=1}^{n}\sum_{l=1}^{n} \frac{1}{\omega_{ij}'\omega_{kl}'} 2^6 \sin(\frac{i\pi x}{a})\sin(\frac{j\pi y}{b})\sin(\frac{k\pi x}{a})\sin(\frac{l\pi y}{b})\sin(\frac{i\pi x_0}{a})\sin(\frac{j\pi y_0}{b})$$

$$\sin(\frac{k\pi x_0}{a})\sin(\frac{l\pi y_0}{b})\int_0^t e^{-\omega_b\tau}\sin(\omega_{ij}'\tau)e^{-\omega_b\tau}\sin(\omega_{kl}'\tau)\sin(\frac{i\pi vt - i\pi v\tau}{a})\sin(\frac{j\pi y}{b})$$

$$\sin(\frac{k\pi vt - k\pi v\tau}{a})\sin(\frac{l\pi y}{b})d\tau \tag{21}$$

As the cross values for *ij # kl* are sufficiently smaller than those for *ij=kl* [30], the cross values for *ij # kl* can be neglected.

$$E[w^2(x,y,t)] = 2\pi S_p \sum_{i=1}^{n}\sum_{j=1}^{n} \frac{1}{\omega_{ij}'^2} 2^6 \sin^2(\frac{i\pi x}{a})\sin^2(\frac{j\pi y}{b})\sin^2(\frac{i\pi x_0}{a})\sin^2(\frac{j\pi y_0}{b})\int_0^t e^{-2\omega_b\tau}$$

$$\sin^2(\omega_{ij}'\tau)\sin^2(\frac{i\pi vt - i\pi v\tau}{a})\sin^2(\frac{j\pi y}{b})d\tau \tag{22}$$

As the *y* component in the assumed moving load is independent of time, it can be deduced to:

$$E[w^2(x,y,t)] = 2\pi S_p \sum_{i=1}^{n}\sum_{j=1}^{n} \frac{1}{\omega_{ij}'^2} 2^4 \sin^2(\frac{i\pi x}{a})\sin^2(\frac{j\pi y}{b})\sin^2(\frac{i\pi x_0}{a})\sin^2(\frac{j\pi y_0}{b})\sin^2(\frac{j\pi y}{b})\int_0^t e^{-2\omega_b\tau}$$

$$(1-\cos(2\omega_{ij}'\tau))(1-\cos(\frac{2(i\pi vt - i\pi v\tau)}{a}))d\tau \tag{23}$$

$$E[w^2(x,y,t)] = \pi S_p \sum_{i=1}^{n}\sum_{j=1}^{n} \frac{1}{\omega_{ij}'^2} 2^4 \sin^2(\frac{i\pi x}{a}) \sin^2(\frac{j\pi y}{b}) \sin^2(\frac{i\pi x_0}{a}) \sin^2(\frac{j\pi y_0}{b}) \sin^2(\frac{j\pi y}{b})$$

$$[\frac{-\omega_b e^{-2\omega_b t}\cos(2\omega_{ij}' t) + \omega_b \cos(-2i\pi v t/a)}{4(\omega_b^2 + (\omega_{ij}' + i\pi v/a)^2)}$$

$$+ \frac{(\omega_{ij}' + i\pi v/a)e^{-2\omega_b t}\sin(2\omega_{ij}' t) - (\omega_{ij}' + i\pi v/a)\sin(-2i\pi v t/a)}{4(\omega_b^2 + (\omega_{ij}' + i\pi v/a)^2)}$$

$$+ \frac{-\omega_b e^{-2\omega_b t}\cos(2\omega_{ij}' t) + \omega_b \cos(2i\pi v t/a)}{4(\omega_b^2 + (\omega_{ij}' - i\pi v/a)^2)}$$

$$+ \frac{(\omega_{ij}' - i\pi v/a)e^{-2\omega_b t}\sin(2\omega_{ij}' t) - (\omega_{ij}' - i\pi v/a)\sin(2i\pi v t/a)}{4(\omega_b^2 + (\omega_{ij}' - i\pi v/a)^2)} + (\frac{1}{-2\omega_b})e^{-2\omega_b t}$$

$$- \frac{-2\omega_b(e^{-2\omega_b t}\cos(2\omega_{ij}' t) - 1) + 2\omega_{ij}'\sin(2\omega_{ij}')}{4(\omega_b^2 + (\omega_{ij}')^2)}$$

$$- \frac{-2\omega_b(e^{-2\omega_b t} - \cos(2i\pi v t/a)) + (-2i\pi v/a)(-\sin(2i\pi v t/a))}{4(\omega_b^2 + (-i\pi v/a)^2)}] \quad (24)$$

For the constant covariance, the covariance and the spectral density are determined as follows:

$$R_{pp}(\tau_1,\tau_2) = \sigma_p^2 \quad , \quad S_{pp}(\omega_1,\omega_2) = 2\pi\sigma_p^2\delta(\omega_2 - \omega_1) \quad (25)$$

where σ_p is a constant value. The squared mean value is achieved as follows:

$$E[w^2(x,y,t)] = \sigma_p^2 \sum_{i=1}^{n}\sum_{j=1}^{n}\sum_{k=1}^{n}\sum_{l=1}^{n} \phi_{ij}(x,y)\phi_{kl}(x,y)\phi_{ij}(x_0,y_0)\phi_{kl}(x_0,y_0)\int_0^t\int_0^t h_{ij}(\tau_1)h_{kl}(\tau_2)\phi_{ij}(vt$$

$$-v\tau_1, y)\phi_{kl}(vt - v\tau_2, y)d\tau_1 d\tau_2 \quad (26)$$

$$E[w^2(x,y,t)] = \sigma_p^2 \sum_{i=1}^{n}\sum_{j=1}^{n}\sum_{k=1}^{n}\sum_{l=1}^{n} \frac{1}{\omega_{ij}'}\frac{1}{\omega_{kl}'} 2^6 \sin(\frac{i\pi x}{a})\sin(\frac{j\pi y}{b})\sin(\frac{k\pi x}{a})\sin(\frac{l\pi y}{b})\sin(\frac{i\pi x_0}{a})\sin(\frac{j\pi y_0}{b})$$

$$\sin(\frac{k\pi x_0}{a})\sin(\frac{l\pi y_0}{b})\int_0^t\int_0^t e^{-\omega_b\tau_1}\sin(\omega_{ij}'\tau_1)e^{-\omega_b\tau_2}\sin(\omega_{kl}'\tau_2)\sin(\frac{i\pi vt - i\pi v\tau_1}{a})\sin(\frac{j\pi y}{b})$$

$$\sin(\frac{k\pi vt - k\pi v\tau_2}{a})\sin(\frac{l\pi y}{b})d\tau_1 d\tau_2 \quad (27)$$

$$E[w^2(x,y,t)] = \sigma_p^2 \sum_{i=1}^{n}\sum_{j=1}^{n} \frac{1}{\omega_{ij}'^2} 2^6 \sin^2(\frac{i\pi x}{a})\sin^2(\frac{j\pi y}{b})\sin^2(\frac{i\pi x_0}{a})\sin^2(\frac{j\pi y_0}{b})\int_0^t\int_0^t e^{-\omega_b\tau_1}\sin(\omega_{ij}'\tau_1)$$

$$e^{-\omega_b\tau_2}\sin(\omega'_{ij}\tau_2)\sin(\frac{i\pi vt-i\pi v\tau_1}{a})\sin(\frac{j\pi y}{b})\sin(\frac{i\pi vt-i\pi v\tau_2}{a})\sin(\frac{j\pi y}{b})d\tau_1 d\tau_2 \tag{28}$$

$$E[w^2(x,y,t)]=\sigma_p^2\sum_{i=1}^{n}\sum_{j=1}^{n}\frac{1}{\omega'^2_{ij}}2^6\sin^2(\frac{i\pi x}{a})\sin^2(\frac{j\pi y}{b})\sin^2(\frac{i\pi x_0}{a})\sin^2(\frac{j\pi y_0}{b})$$

$$[\frac{-\omega_b e^{-\omega_b t}\cos(\omega'_{ij}t)+\omega_b\cos(-i\pi vt/a)}{2(\omega_b^2+(\omega'_{ij}+i\pi v/a)^2)}$$

$$+\frac{(\omega'_{ij}+i\pi v/a)e^{-\omega_b t}\sin(\omega'_{ij}t)-(\omega'_{ij}+i\pi v/a)\sin(-i\pi vt/a)}{2(\omega_b^2+(\omega'_{ij}+i\pi v/a)^2)}$$

$$-\frac{-\omega_b e^{-\omega_b t}\cos(\omega'_{ij}t)+\omega_b\cos(i\pi vt/a)}{2(\omega_b^2+(\omega'_{ij}-i\pi v/a)^2)}$$

$$-\frac{(\omega'_{ij}-i\pi v/a)e^{-\omega_b t}\sin(\omega'_{ij}t)-(\omega'_{ij}-i\pi v/a)\sin(i\pi vt/a)}{2(\omega_b^2+(\omega'_{ij}-i\pi v/a)^2)} \tag{29}$$

For the exponential cosine, the covariance and the spectral density are determined based on what follows:

$$R_{pp}(\tau_1,\tau_2)=\sigma_p^2 e^{-\omega_g|\tau_2-\tau_1|}\cos(\omega_0\tau_2-\omega_0\tau_1),\ S_{pp}(\omega_1,\omega_2)=\sigma_p^2\omega_g[1/\{\omega_g^2+(\omega+\omega_0)^2\}+1/\{\omega_g^2+(\omega-\omega_0)^2\}] \tag{30}$$

where σ_p, ω_g, and ω_0 are constants. The squared mean value is attained as:

$$E[w^2(x,y,t)]=\sigma_p^2\sum_{i=1}^{n}\sum_{j=1}^{n}\sum_{k=1}^{n}\sum_{l=1}^{n}\phi_{ij}(x,y)\phi_{kl}(x,y)\phi_{ij}(x_0,y_0)\phi_{kl}(x_0,y_0)\int_0^t\int_0^t h_{ij}(\tau_1)h_{kl}(\tau_2)\phi_{ij}(vt$$

$$-v\tau_1,y)\phi_{kl}(vt-v\tau_2,y)e^{-\omega_g|\tau_2-\tau_1|}\cos(\omega_0\tau_2-\omega_0\tau_1)d\tau_1 d\tau_2 \tag{31}$$

$$E[w^2(x,y,t)]=\sigma_p^2\sum_{i=1}^{n}\sum_{j=1}^{n}\sum_{k=1}^{n}\sum_{l=1}^{n}\frac{1}{\omega'_{ij}}\frac{1}{\omega'_{kl}}2^6\sin(\frac{i\pi x}{a})\sin(\frac{j\pi y}{b})\sin(\frac{k\pi x}{a})\sin(\frac{l\pi y}{b})\sin(\frac{i\pi x_0}{a})\sin(\frac{j\pi y_0}{b})$$

$$\sin(\frac{k\pi x_0}{a})\sin(\frac{l\pi y_0}{b})\int_0^t\int_0^t e^{-\omega_b\tau_1}\sin(\omega'_{ij}\tau_1)e^{-\omega_b\tau_2}\sin(\omega'_{kl}\tau_2)\sin(\frac{i\pi vt-i\pi v\tau_1}{a})\sin(\frac{j\pi y}{b})$$

$$\sin(\frac{k\pi vt-k\pi v\tau_2}{a})\sin(\frac{l\pi y}{b})e^{-\omega_g|\tau_2-\tau_1|}\cos(\omega_0\tau_2-\omega_0\tau_1)d\tau_1 d\tau_2 \tag{32}$$

$$E[w^2(x,y,t)]=\sigma_p^2\sum_{i=1}^{n}\sum_{j=1}^{n}\sum_{k=1}^{n}\sum_{l=1}^{n}\frac{1}{\omega'_{ij}}\frac{1}{\omega'_{kl}}2^6\sin(\frac{i\pi x}{a})\sin(\frac{j\pi y}{b})\sin(\frac{k\pi x}{a})\sin(\frac{l\pi y}{b})\sin(\frac{i\pi x_0}{a})\sin(\frac{j\pi y_0}{b})$$

$$\sin(\frac{k\pi x_0}{a})\sin(\frac{l\pi y_0}{b})\int_0^t[\int_0^{\tau_1}e^{-\omega_b\tau_1}\sin(\omega'_{ij}\tau_1)e^{-\omega_b\tau_2}\sin(\omega'_{kl}\tau_2)\sin(\frac{i\pi vt-i\pi v\tau_1}{a})\sin(\frac{j\pi y}{b})\sin(\frac{k\pi vt-k\pi v\tau_2}{a})$$

$$\sin(\frac{l\pi y}{b})e^{-\omega_g(\tau_1-\tau_2)}\cos(\omega_0\tau_2-\omega_0\tau_1)d\tau_2+\int_{\tau_1}^{t}e^{-\omega_b\tau_1}\sin(\omega'_{ij}\tau_1)e^{-\omega_b\tau_2}\sin(\omega'_{kl}\tau_2)\sin(\frac{i\pi vt-i\pi v\tau_1}{a})\sin(\frac{j\pi y}{b})$$

$$\sin(\frac{k\pi vt-k\pi v\tau_2}{a})\sin(\frac{l\pi y}{b})e^{-\omega_g(\tau_2-\tau_1)}\cos(\omega_0\tau_2-\omega_0\tau_1)d\tau_2]d\tau_1 \quad (33)$$

$$E[w^2(x,y,t)]=\sigma_p^2\sum_{i=1}^{n}\sum_{j=1}^{n}\frac{1}{\omega'^2_{ij}}2^6\sin^2(\frac{i\pi x}{a})\sin^2(\frac{j\pi y}{b})\sin^2(\frac{i\pi x_0}{a})\sin^2(\frac{j\pi y_0}{b})\sin^2(\frac{j\pi y}{b})$$

$$\int_0^t[\int_0^{\tau_1}e^{-\omega_b\tau_1}\sin(\omega'_{ij}\tau_1)e^{-\omega_b\tau_2}\sin(\omega'_{ij}\tau_2)\sin(\frac{i\pi vt-i\pi v\tau_1}{a})\sin(\frac{i\pi vt-i\pi v\tau_2}{a})e^{-\omega_g(\tau_1-\tau_2)}\cos(\omega_0\tau_2-\omega_0\tau_1)d\tau_2$$

$$+\int_{\tau_1}^{t}e^{-\omega_b\tau_1}\sin(\omega'_{ij}\tau_1)e^{-\omega_b\tau_2}\sin(\omega'_{ij}\tau_2)\sin(\frac{i\pi vt-i\pi v\tau_1}{a})\sin(\frac{i\pi vt-i\pi v\tau_2}{a})e^{-\omega_g(\tau_2-\tau_1)}\cos(\omega_0\tau_2-\omega_0\tau_1)d\tau_2]d\tau_1 \quad (34)$$

$$E[w^2(x,y,t)]=\sigma_p^2\sum_{i=1}^{n}\sum_{j=1}^{n}\frac{1}{\omega'^2_{ij}}2^6\sin^2(\frac{i\pi x}{a})\sin^2(\frac{j\pi y}{b})\sin^2(\frac{i\pi x_0}{a})\sin^2(\frac{j\pi y_0}{b})\sin^2(\frac{j\pi y}{b})$$

$$\int_0^t[\int_0^{\tau_1}\sin(\omega'_{ij}\tau_1)\sin(\omega'_{ij}\tau_2)\sin(\frac{i\pi vt-i\pi v\tau_1}{a})\sin(\frac{i\pi vt-i\pi v\tau_2}{a})e^{-\omega_g(\tau_1-\tau_2)-\omega_b(\tau_1+\tau_2)}\cos(\omega_0\tau_2-\omega_0\tau_1)d\tau_2$$

$$+\int_{\tau_1}^{t}\sin(\omega'_{ij}\tau_1)\sin(\omega'_{ij}\tau_2)\sin(\frac{i\pi vt-i\pi v\tau_1}{a})\sin(\frac{i\pi vt-i\pi v\tau_2}{a})e^{-\omega_g(\tau_2-\tau_1)-\omega_b(\tau_1+\tau_2)}\cos(\omega_0\tau_2-\omega_0\tau_1)d\tau_2]d\tau_1 \quad (35)$$

The all governing formulas of the exponential cosine covariance, are converted to the exponential and the cosine wave covariance by limiting the ω_0 and ω_g to zero respectively.

In the rectangular plate with the surface constant crack case, while the mode shape of the plate must consider the plate's boundary conditions form and can satisfy the differential equation, according to the Ritz method, the mode shape is represented as the two sets of the functions' summation:

$$\phi_{ij}(x,y)=\phi_{ij_p}(x,y)+\phi_{ij_c}(x,y) \quad (36)$$

where, $\phi_{ij_p}(x,y)$ denotes the behavior of the intact plate, in which:

$$\phi_{ij_p}(x,y)=\sum_{i=1}^{N}\sum_{j=1}^{N}a_{ij}\psi_{ij}(x,y) \quad (37)$$

where $\psi_{ij}(x, y)$ is a set of orthogonal polynomials in x and y directions, directed in the plate's edges directions, generated by the Gram-Schmidt process [31], expressed according to the boundary characteristics orthogonal polynomials (BCOP) method [32]. N is the number of utilized orthogonal polynomials, and a_{ij} is a set of constants, indicating the participation ratio of the orthogonal polynomials.

$\phi_{ij_c}(x,y)$ are the William's solutions for the plate's internal crack, denoted the well-known corner functions, expressing behavior of the cracked plate along the crack line as additional modes, additionally, $\phi_{ij_c}(x,y)$ described the stress singularity near the tips of the crack and the discontinuities along the crack [33]:

$$\phi_{ij_c}(x,y) = x^{n_1}(a-x)^{n_2}\, y^{n_3}(b-y)^{n_4}\{\sum_{n=1}^{N_1} b_n \phi_{n,S}(\gamma_n, r_1, \theta_1, r_2, \theta_2) + \sum_{n=1}^{N_2} c_n \phi_{n,A}(\gamma_n, r_1, \theta_1, r_2, \theta_2)$$

$$+\sum_{n=1}^{N_3} c_n \phi_{n,A}(\gamma_n, r_1, \theta_1, r_2, \theta_2) + \sum_{n=1}^{N_4} e_n \phi_{n,S}(\gamma_n, r_2, \theta_2, r_1, \theta_1)\} \quad (38)$$

in which:

$$\gamma_n = n/2 \quad , \quad n = 1, 2, \ldots \quad (39-a)$$

and for $\gamma_n \in \mathrm{N}$ (natural numbers):

$$\phi_{n,S}(\gamma_n, r_1, \theta_1, r_2, \theta_2) = r_j^{\bar{k}} r_i^{\gamma_n+1}(-\frac{\lambda_2}{\lambda_1}\cos(\gamma_n+1)\theta_i + \cos(\gamma_n-1)\theta_i) \quad (39-b)$$

$$\phi_{n,A}(\gamma_n, r_1, \theta_1, r_2, \theta_2) = r_j^{\bar{k}} r_i^{\gamma_n+1}(\frac{\lambda_3}{\lambda_1}\sin(\gamma_n+1)\theta_i + \sin(\gamma_n-1)\theta_i) \quad (39-c)$$

and for $\gamma_n \notin \mathrm{N}$ (natural numbers):

$$\phi_{n,S}(\gamma_n, r_1, \theta_1, r_2, \theta_2) = \sin^2(\theta_j/2) r_j^k r_i^{\gamma_n+1}(\frac{\lambda_3}{\lambda_1}\cos(\gamma_n+1)\theta_i + \cos(\gamma_n-1)\theta_i) \quad (39-d)$$

$$\phi_{n,A}(\gamma_n, r_1, \theta_1, r_2, \theta_2) = \sin^2(\theta_j/2) r_j^k r_i^{\gamma_n+1}(-\frac{\lambda_2}{\lambda_1}\sin(\gamma_n+1)\theta_i + \sin(\gamma_n-1)\theta_i) \quad (39-e)$$

where

$$\lambda_1 = (\gamma_n+1)(\nu+1)\ ,\ \lambda_2 = -\gamma_n(1-\nu) + (3+\nu)\ ,\ \lambda_3 = \gamma_n(1-\nu) + (3+\nu) \quad (39-f)$$

The polar coordinates (r_1, θ_1) and (r_2, θ_2) are the two tips of an internal crack. The subscripts *A* and *S* indicate asymmetric and symmetric modes respectively. n_1, n_2, n_3, and n_4 represent the boundary conditions of the cracked plate. There are three geometrical boundary conditions, namely clamped, simply supported and free. N_1, N_2, N_3, and N_4 are the number of the admissible corner functions. b_n, c_n, d_n, and e_n are the constants, expressing the participation ratio of the admissible corner functions.

3. Validation Process and the numerical results of the present study

The numerical results are presented as the time-dependent behavior of the function of the squared mean value at any point with x_0 and y_0 coordinates in the rectangular or square-shaped thin intact and cracked plates, for several load velocities, and for five covariance patterns of the moving random load, scilicet the white noise, constant, exponential cosine, exponential and the cosine wave covariance. The non-dimensional function of the squared mean value (the function of z), the non-dimensional speed parameter, and the non-dimensional damping parameter are determined as follows, respectively:

$$y(z) = \frac{E[w^2(x,y,t)]}{w_0 V_p}\ ,\ z = x/a\ ,\ 0 \le z \le 1 \quad (40)$$

where a is the length of the plate, w_0 is the deflection at the middle of the plate due to the static load P, and the coefficient V_p is determined for the white noise as $V_p = \sqrt{S_p} / P$ and for the other four covariance as $V_p = \sigma_p / P$.

$$\alpha = \pi v / a\omega \tag{41}$$

where ω is the natural frequency of the intact plate or the cracked plate. Therefore, $0 \le \alpha \le 1$.

$$\beta = \omega_b / \omega \tag{42}$$

According to the designated damping coefficient, β = 0, 0.1. The non-dimensional parameters g and γ are introduces respectively:

$$g = \omega_g a / v \quad , \quad \gamma = \omega_0 a / v \tag{43}$$

For limiting the g, γ and both g and γ to zero, deduced the cosine wave, exponential and constant covariance cases respectively. The g and γ are determined the covariance specifies, designated as g = 0, 0.1, γ = 0, π/α.

While the moving random loads are passed through the middle of plates, the y coordinate is always constant and accordingly, the functions of z at the middle point of a simply-supported intact rectangular plate can be compared with the functions of z at the middle point of a simply-supported beam, obtained by Fryba [4,28]. Therefore, in the following figures, first, the functions of z at the middle point of a simply-supported intact rectangular plate subjected to the moving random load with the mentioned patterns, namely the white noise, constant, and the exponential cosine, are compared with the functions of z at the middle point of a simply-supported beam subjected to the same moving random loads, and after verifications of the convergence and the accuracy of presented method, the numerical results of cracked plates are presented and the parametric studies are carried out.

Figures 1 to 3 reveal the functions of z at the middle point of a simply-supported intact rectangular plate subjected to the moving random loads in comparison with those of a simply-supported beam subjected to the same loads. As Figures illustrate, only due to the constant parameters in plates and beam, such as the plate's flexural rigidity and the constant bending stiffness of the beam, there is a measure difference between the results. As the equation (40) reveals, the function of z is function of the squared deflections. Besides the partial differential equation of motion of a uniform thin rectangular plate, subjected to a moving load in equation (1) shows the effect of the plate's flexural rigidity on the deflection. In other side the partial differential equation of motion of a Bernoulli-Euler Beam, subjected to a moving load, is described as follow [27]:

$$EI\nabla^4 W(x,t) + c\frac{\partial W(x,t)}{\partial t} + m\frac{\partial^2 W(x,t)}{\partial t^2} = P(x,t) = \delta(x - x_0)P(t) \tag{44}$$

where $W(x, t)$ is the vertical deflection of the Beam at any time-dependent coordinates x. $EI = \frac{Ebh^3}{12}$, is the constant bending stiffness of the beam, where E, b, and h are the beam's modulus of elasticity, width and thickness, respectively. Accordingly, m, and c are the mass per unit area and damping constant of the beam respectively. Therefore, the beam's deflection depends on $\frac{1}{EI}$ and accordingly the beam's squared deflection depends on $(\frac{1}{EI})^2$. By making the equation dimensionless, the functions of z of a beam depend on $(\frac{12}{E})^2$. while the assumed moving random loads are passed through the middle of plates, the y coordinate is always constant, therefore, the plate's deflection depends on x coordinate similar to the beam and accordingly depends on $\frac{1}{D}$ where $D = \frac{Eh^3}{12(1-\nu^2)}$, is the

plate's flexural rigidity and consequently, the plate's squared deflection depends on $(\frac{1}{D})^2$. By making the equation dimensionless, the function of z of plate depend on $(\frac{12(1-\nu^2)}{E})^2$. Therefore, by utilizing alike materials for beams and plates, the function of z of the plate and the function of z of the beam differ by $(1-\nu^2)^2$. In the presented investigation, the simply–supported aluminum thin square plate with the mass density ρ = 2700 kgm^{-3}, the modulus of elasticity E = 7.31× 10^{10} pa, and the Poisson's ratio ν = 0.33, for the convergence study, are taken into consideration. The designated width and the length of the plate are equal to 2 m and its thickness is 1.7 cm [26]. Of course, according to the non-dimensional function, only the Poisson's ratio is included in the calculations.

Figure 1 shows the functions of z at the middle point of a simply-supported intact rectangular plate subjected to the moving random load with the white noise covariance with various speed parameters in comparison with those of a simply-supported beam.

Figure 2 demonstrates the functions of z at the middle point of a simply-supported intact rectangular plate subjected to the moving random load with the constant covariance with various speed parameters in comparison with those of a simply-supported beam subjected to the same loads.

Figure 3 shows the functions of z at the middle point of a simply-supported intact rectangular plate subjected to the moving random load with the exponential cosine covariance with various speed parameters in comparison with those of a simply-supported beam subjected to the same loads.

After attesting the convergence and the accuracy of the proposed method, the investigation of the moving random load effect and the parametric studies of the cracked plates, are performed. Since studied cracks, are constant cracks [34], increasing the inclined crack angles as well as the crack lengths are extended to the limitation that stress intensity factors should be less than the critical stress intensity factor [34]. The limitation of moving load velocities and magnitudes are depended on the plates' dynamic stability, conformed to the characteristic equation or the frequency equation [35], the positive root for plates natural frequencies, the positive definition of the plates' masses as well as the plates stiffness. As the following diagrams are presented as non-dimensional diagrams, the moving load velocities and magnitude are not considered directly in the diagrams. In other words, the moving load magnitude is not included in the calculations. Besides the dynamic responses are investigated until the moving load is on the plate and due to the simple-supported plate natural frequencies formula, presented by Leissa [36] as $\omega_n = \omega_{ij} = \pi^2[(\frac{i}{a})^2 + (\frac{j}{b})^2]\sqrt{\frac{D}{m}}$, the designated dimensions of the plate and the definition of the speed parameter α, the moving load velocities are in any case in the plate's dynamic stability limitation.

Figure 4 to 8 illustrate behavior of the functions of z at the middle point of the damped and undamped intact rectangular plates as well as the damped and undamped rectangular plates with a surface constant crack at the middle of the plates subjected to the moving random load, passed through the middle of plates, with five different covariance, the white noise, the constant covariance, the exponential cosine, the exponential and the cosine wave covariance.

Figure 4 exhibits the functions of z at the middle of the undamped and damped intact plates and the cracked plates with the crack length equal to c/a = 0.5 and the 45° inclined crack angle, subjected to the moving random load with the white noise covariance with different speed parameters. By increasing the non-dimensional time parameter (i.e. z), the function of z in the undamped cracked plate case compared with the undamped intact plate case, for the speed parameter 0.25, increases substantially and for the other speed parameters, increases gradually because of the crack presence and the moving random load effect. The order of speed parameters in the denominator of the squared mean value equation, deduced the functions of z, is larger than the order of speed parameters in the numerator of that function, accordingly, the function of z in the undamped cracked plate case in comparison with the undamped intact plate case, for the speed parameter 0.25, is increase excessively, compared to that for the other speed parameters. The increasing of the function of z in the damped cracked plate cases compared to the damped intact plate cases is similar to the increasing the undamped cracked plate cases compared to the undamped intact plate cases although the

increasing is more moderately than those in the undamped cases due to the damper. Furthermore, in the mentioned damped intact and cracked plate cases, for the speed parameter equal to zero, the maximum functions of z appear when the moving load arrives near to the middle of the plates and in all other cases, those appear when the moving load comes nearby the right side of the plates. The function of z illustrates the function of the dynamic deflection to the static deflection ratio. Therefore, the maximum ratio's function in the white noise covariance case, in the damped intact and cracked plate case is a bet less than 1.5 at the speed parameter zero and in the undamped intact and cracked plate case is a bit more than 1.5 at the speed parameter 0.5.

Figure 5 show the behavior of the functions of z in time, at the middle point of the damped and undamped cracked plates with the crack length equal to c/a = 0.5 and the 45° inclined crack angle, as well as the damped and undamped intact plates, subjected to the moving random load with constant covariance. As shown in Figure 5, due to the admissible corner functions, in the cracked plate cases, the functions of z in that case are higher than those in the intact plate cases. The functions of z in the undamped cracked plate cases are larger than those of the damped cracked plate cases because of the damping. Moreover, in the alluded damped intact and cracked plate cases, for the speed parameter equal to zero and 1, the maximum functions of z appear when the moving load arrives near to the middle of the plates and nearby the right side of the plates respectively. Those events are similar to the white noise covariance case. In the other hand, in the mentioned damped intact and cracked plate cases, for the speed parameter 0.25 and 0.5, the maximum functions of z reach when the moving load comes nearby 40% of the left side distance of the plates and 35% of the right side distance of the plates respectively. The maximum dynamic deflection to the static deflection ratio's function in the constant covariance case, in the damped and undamped intact and cracked plate case is a bet less than 1.5 at the speed parameter 0.5.

Figure 6 illustrate the effect of the crack line to the functions of z at the middle point of the undamped and damped intact as well as cracked plates with the crack length equal to c/a = 0.5 and the 45° inclined crack angle, subjected to the moving random load with exponential cosine covariance. The alteration of the functions of z, caused by cosine component, is large enough, that the modifying, created by exponential component, is covered and the increasing of the functions of z due to the crack line seem insignificant. It can be observed that, while the damping component, appears as a negative power in the exponential component, increase in the functions of z, caused by admissible corner functions, in the damped cracked plate case, is greater than those in the undamped cracked plate case. Besides, in the mentioned damped intact and cracked plate cases, for the speed parameter equal to zero, the maximum functions of z reach when the moving load arrives near to the middle of the plates and in all other cases, those appear when the moving load comes nearby the right side of the plates. Those events are similar to the white noise covariance case. The maximum dynamic deflection to the static deflection ratio's function in the exponential cosine covariance case, in the damped intact and cracked plate case is a bet more than 4 at the speed parameter zero and in the undamped intact and cracked plate case is a bit more than 3 at the speed parameter 0.25.

Figure 7 reveal the functions of z at the middle point of the undamped and damped crack plates with the crack length equal to c/a = 0.5 and the 45° inclined crack angle, in comparison with those of the intact plates, subjected to the moving random load with exponential covariance pattern. Due to the crack line, the functions of z in the undamped and damped crack plate cases are greater than those in the undamped and damped intact plate cases. As the equation (30) reveals, the exponential covariance, derives by limiting the ω_0 to zero. Therefore, the damping element, expressed as a negative power in the exponential element. Accordingly, the increase of the functions of z due to the crack line in the damped crack plate cases, is greater than those in the undamped crack plate cases. Otherwise, in the mentioned damped intact and cracked plate cases, for the speed parameter equal to zero and 1, the maximum functions of z reach when the moving load arrives near to the middle of the plates and nearby the right side of the plates respectively. Further, in the mentioned damped intact and cracked plate cases, for the speed parameter 0.25 and 0.5, the maximum functions of z reach when the moving load comes nearby 40% of the left side distance of the plates and 35% of the right side distance of the plates respectively. Those events are similar to the constant covariance case. The maximum dynamic deflection to the static deflection ratio's function in the exponential covariance case, in the undamped intact and cracked plate case is a bet less than 1.5 at the speed parameter 0.5 and in the damped intact plate case is a bet less than 1.5 at the speed parameter 0.5 however in the damped cracked plate case is a bit less than 1.5 at the speed parameter 0.25.

Figure 8 illustrate, the increasing trend of the functions of z at the middle point of the undamped and damped cracked plates with the crack length equal to c/a = 0.5 and the 45° inclined crack angle, subjected to the moving random load with cosine covariance, versus those of the undamped and damped intact plates. As the equation (30) reveals, the cosine covariance derives by limiting the ω_g to zero. As the high values of the functions of z in the cosine wave covariance cases reveal, the effect of the cosine component prevails in the all other components, such as the admissible corner functions in the cracked plates. Accordingly, the increase in the functions of z in the undamped and damped cracked plate cases in comparison with the undamped and damped of intact plate cases are inconsiderable. In addition, in the alluded damped intact and cracked plate cases, for the speed parameter equal to zero, the maximum functions of z reach when the moving load arrives near to the middle of the plates and in all other cases, those appear when the moving load comes nearby the right side of the plates. Those events are similar to the white noise as well as exponential cosine covariance case. The maximum dynamic deflection to the static deflection ratio's function in the cosine covariance case, in the damped intact and cracked plate case is a bet more than 4 at the speed parameter zero and in the undamped intact and cracked plate case is a bit more than 3 at the speed parameter 0.25.

Consequently, the proposed method can be utilized to obtain behaviors of the functions of z in undamped and damped plate with more than one crack in various locations.

Figure 9 illustrates the behaviors of the functions of z at the middle point of the damped plate with the crack length equal to 0.4 of the plate length with the inclined crack angle equal to 30°, located in the middle of the plate, versus those that located in the corner of the plate, subjected to the moving random load with three different covariance patterns, including the white noise, constant covariance, and the exponential cosine covariance. In addition, the behaviors of the functions of z at the middle point of the damped plate with the crack length equal to 0.4 of the plate length with the inclined crack angle equal to 30°, located in the corner of the plate, are compared with functions of z at the middle point of the damped plate with the crack length equal to 0.5 of the plate length with the inclined crack angle equal to 45°, located in the middle of the plate, in comparison with the functions of z at the middle point of the damped plate with the total of mentioned cracks subjected to the moving random load with various speed parameters and three different covariance patterns, scilicet the white noise, constant, and the exponential covariance. As figures show, the functions of z at the middle point of the damped plate with the total of mentioned cracks, are a little more than the functions of z at the middle point of the damped plate with mentioned cracks individually.

In the following, parametric studies are implement to indicate effects of the crack lengths, and the inclined crack angles, on the functions of z at the middle point of the plates with a surface constant crack at the middle of the plates subjected to the moving random load, passed through the middle of plates. As Figure 10 to 19 demonstrate, the effects of the crack lengths, and the inclined crack angles, on the functions of z at the middle point of the cracked plates subjected to the moving random load are gently because the crack is assumed as a constant crack. Besides, there are non-monotonous nonlinear relations between the plates' functions of z and the inclined crack angles as well as the crack lengths in all cases.

Figure 10 reveals the effects of the inclined crack angles on the functions of z at the middle point of the undamped and damped cracked plates, subjected to the moving random load with the white noise covariance pattern with various speed parameters at the constant distance parameters. For the moving random load, at the distance parameters $z = 0.3\ z`$, $z = 0.5\ z`$, in all undamped and damped cracked plate cases, and for the moving random load at the distance parameter $z = 0.7\ z`$, in all damped cracked plate cases, and the undamped cracked plate cases with speed parameters $\alpha = 0.5$, and $\alpha = 1$, the inclinations of the relevant curves grow insignificant, while for the moving random load at the distance parameter $z = 0.7\ z`$, in the undamped cracked plate cases with speed parameters $\alpha = 0.25$, increase gently. According to the white noise function of z formula and the admissible corner function formulation, the modified parameters due to the inclined crack angles modifying, are much less than one. Therefore, the effects of the inclined crack angles on the functions of z in all cases, are not significant.

Figure 11 illustrates the effects of inclined crack angles on the functions of z at the middle point of the undamped and damped cracked plates, subjected to the moving random load with the constant covariance pattern with various speed parameters at the constant distance parameters. For moving random load at the distance parameters $z = 0.3z`$, with the speed parameter $\alpha = 0.25$, in the undamped and damped cracked plate cases, for moving random load at the

distance parameter $z = 0.5\ z`$, with the speed parameter $\alpha = 0.25$, in the undamped and damped cracked plate cases and speed parameter $\alpha = 0.5$, in the damped cracked plate cases, as well as for moving random load at the distance parameter $z = 0.7\ z`$, with the speed parameters $\alpha = 0.25$, and $\alpha = 0.5$ in the undamped and damped cracked plate cases, the inclinations of the relevant curves grow moderately while in all other cases, increase inconsiderably. In conformity with the constant function of z formulation and the admissible corner function formula, the varied parameters due to the inclined crack angles varying, used in that value, are less than one, multiplied by less than one. Accordingly, the consequences of the inclined crack angles modifying on the functions of z in all cases, are not effective.

Figure 12 shows the effects of inclined crack angles on the functions of z at the middle point of the undamped and damped cracked plates, subjected to the moving random load with the exponential cosine covariance pattern with various speed parameters at the constant distance parameters. In all cases, the inclinations of the relevant curves grow slightly. According to the exponential cosine function of z formula and the admissible corner function formulation, the cosine factor overshadows modified parameters due to the inclined crack angles alteration, used in that value. Therefore, the effects of inclined crack angles on the functions of z in all cases, are insignificant.

Figure 13 illustrates effects of inclined crack angles on the functions of z at the middle point of the undamped and damped cracked plates, subjected to the moving random load with the exponential covariance with various speed parameters at the constant distance parameters. For moving random load at the distance parameters $z = 0.3z`$, $z = 0.5z`$, and $z = 0.7z`$, with the speed parameter $\alpha = 0.25$, in the undamped cracked plate cases, for moving random load at the distance parameters $z = 0.3z`$, and $z = 0.7z`$, with the speed parameter $\alpha = 0.25$, and $\alpha = 1$, in damped cracked plate cases, for moving random load at the distance parameters $z = 0.5z`$, and $z = 0.7z`$, with the speed parameter $\alpha = 0.5$, and $\alpha = 1$, in damped cracked plate cases, the inclinations of the relevant curves, for more than 15° inclined crack angles, increase considerably while in all other cases, increase insignificantly.

Figure 14 elucidates effects of inclined crack angles on the functions of z at the middle point of the undamped and damped cracked plates, subjected to the moving random load with the cosine wave covariance with various speed parameters at the constant distance parameters. For all cases, the inclinations of the relevant curves increase inconsiderably. According to the cosine function of z formula and the admissible corner function formulation, the modifying of that value due to the inclined crack angles variation, is covered by cosine component effect. Therefore, the effects of the inclined crack angles on the functions of z in all cases, are insignificant.

Figure 15 reveals effects of crack lengths on the functions of z at the middle point of the undamped and damped cracked plates, subjected to the moving random load with the white noise covariance with various speed parameters at the constant distance parameters. For moving random load, at the distance parameters $z = 0.3\ z`$, $z = 0.5\ z`$, and $z = 0.7\ z`$, with speed parameters $\alpha = 0$, in the damped cracked plate cases, the inclinations of the relevant curves grow moderately, while in all other cases, increase slightly. In conformity with the white noise function of z formulation and the admissible corner function formula, the altered parameters due to the crack lengths modifying, used in that value, are less than one because the crack is assumed as a constant crack. Accordingly, the consequences of crack lengths varying on the functions of z, are moderately.

Figure 16 indicates effects of crack lengths on the functions of z at the middle point of the undamped and damped cracked plates, subjected to the moving random load with the constant covariance with various speed parameters at the constant distance parameters. For moving random load, at the distance parameters $z = 0.3\ z`$, $z = 0.5\ z`$, and $z = 0.7\ z`$, with speed parameters $\alpha = 0.25$, in the undamped cracked plate cases, the inclinations of the relevant curves, for the crack length less than 0.3a increase gently, while in all other cases, increase insignificantly. According to the constant function of z formula and the admissible corner function formulation, the modified parameters due to the crack lengths varying, used in that value, are less than one because the crack is assumed as a constant crack. Therefore, the crack lengths moderately affect the functions of z.

Figure 17 illustrates effects of crack lengths on the functions of z at the middle point of the undamped and damped cracked plates, subjected to the moving random load with the exponential cosine covariance with various speed parameters at the constant distance parameters. The inclinations of the relevant curves grow inconsiderably. In conformity with the exponential cosine function of z formula and the admissible corner function formulation, the

cosine factor overshadows varied parameters due to the crack lengths' modification, used in that value because the crack is assumed as a constant crack. Accordingly, the crack lengths gradually affect the functions of z.

Figure 18 shows effects of crack lengths on the functions of z at the middle point of the undamped and damped cracked plates, subjected to the moving random load with the exponential covariance with various speed parameters at the constant distance parameters. For moving random load, at the distance parameters $z = 0.3\ z`$, $z = 0.5\ z`$, and $z = 0.7\ z`$, with speed parameters $\alpha = 0$, in the undamped and damped cracked plate cases, the inclinations of the relevant curves, for the crack length less than 0.1a grow moderately, while in all other cases, increase insignificantly. According to the exponential function of z formulation and the admissible corner function formula, the modified parameters due to the crack lengths variation, affect to alter that value. While the crack is assumed as a constant crack, the effects of the crack lengths on the functions of z, are moderate.

Figure 19 shows effects of crack lengths on the functions of z at the middle point of the undamped and damped cracked plates, subjected to the moving random load with the cosine wave covariance with various speed parameters at the constant distance parameters. For moving random load, in all cases, the inclinations of the relevant curves grow slightly. In conformity with the cosine function of z formula and the admissible corner function formulation, the varying of that values due to the crack lengths' alterations, are covered by the cosine component effect because the crack is assumed as a constant crack. Accordingly, the crack lengths gently affect the functions of z.

4. Conclusions

The transverse vibration of a thin plate with a surface constant crack at the middle of the plate, subjected to a moving non-stationary random load with a constant velocity and a constant mean value, is systematically investigated. For this purpose, five different covariance patterns are utilized, including videlicet the white noise, constant, exponential, cosine wave and the exponential cosine covariance. The behavior of the functions of z, as the non-dimensional deflection values, at the middle point of the undamped and damped intact as well as cracked plates subjected to the mentioned moving random load, are obtained. The famous corner functions are utilized to express the crack line and two tips of the crack. Based on the obtained results, there are non-monotonous nonlinear relations between the plates' functions of z and the inclined crack angles as well as the crack lengths in all cases. While cracks are to be constant, the functions of z modifications due to the inclined crack angles increase and also, the crack lengths, are moderately developed in all cases. The results obtained from the parametric studies reveal that for the white noise covariance pattern, the modified parameters due to the increase in the inclined crack angles and the crack lengths, are much less than one. Accordingly, the functions of z modify gently. For the constant covariance, the moderated parameters due to the increase in the inclined crack angles and the crack lengths, are more less than one. Therefore, the functions of z vary gradually. For exponential cosine covariance as well as cosine wave covariance, the cosine factor overshadows the altered parameters due to the increase in the inclined crack angles and the crack lengths. Accordingly, the functions of z modify moderately. For the exponential covariance, the functions of z modify significantly due to increase in the inclined crack angles and the crack lengths. In the mentioned damped intact and cracked plate cases, for the speed parameter equal to zero, the maximum functions of z appear when the moving load arrives near to the middle of the plates in all covariance cases, and for other speed parameters in the white noise, cosine and exponential cosine covariance pattern cases, those appear when the moving load comes nearby the right side of the plates. Besides, in the constant and exponential covariance pattern cases, for the speed parameter 1, the maximum functions of z appear when the moving load arrives near to the right side of the plates and for the speed parameter 0.25 and 0.5, those reach when the moving load comes nearby 40% of the left side distance of the plates and 35% of the right side distance of the plates respectively.

The mentioned analyses are idealized for dynamic analyses in recent years' highway and railway transport structures, where flow high weight and speed vehicles.

References

1. Crandall, S.H. "Random vibration", M.I.T. Press, Cambridge, Mass. & John Wiley, New York (1958).
2. Priestley, M.B. "Evolutionary spectra and non-stationary processes", Journal of the Royal Statistical Society: Series B, **27**, pp. 204 – 237 (1965).
3. Priestly, M.B. "Power spectral analysis of non – stationary random processes", Journal of sound and vibration, **6**, pp. 86 – 97 (1967).

4. Fryba, L. “Non-stationary response of a beam to a moving random force”, Journal of Sound and Vibration **46**(3), pp. 323 – 338 (1976).
5. Sniady, P. “Vibration of a beam due to a random stream of moving forces with random velocity”, Journal of Sound and Vibration **97**(1), pp. 23 – 33 (1984).
6. Sieniawska, R., Sniady, P. “First passage problem of the beam under a random stream of moving forces”, Journal of Sound and Vibration **136**(2), pp. 177 – 185 (1990).
7. Sniady, P., Biernat, S., Sieniawska, R., Zukowski, S. “Vibrations of the beam due to a load moving with stochastic velocity”, Probabilistic Engineering Mechanics, **16**, pp. 53 – 59 (2001).
8. Rystwej, A., Sniady, P. “Dynamic response of an infinite beam and plate to a stochastic train of moving forces”, Journal of Sound and Vibration **299**, pp. 1033 – 1048 (2007).
9. Malara, G., Spanos, P.D. “Nonlinear random vibrations of plates endowed with fractional derivative elements”, Probabilistic Engineering Mechanics, **54**, pp. 2 – 8 (2018).
10. Sniady, P., Podworna, M., Idzikowski, R. “Stochastic vibrations of the Euler-Bernoulli beam based on various versions of the gradient nonlocal elasticity theory”, Probabilistic Engineering Mechanics, **56**, pp. 27 – 34 (2019).
11. Kong, F., Spanos, P.D. “Response spectral density determination for nonlinear systems endowed with fractional derivatives and subject to colored noise”, Probabilistic Engineering Mechanics, **59**, art. 103023 (2020).
12. Jiao, Y., Spanos, P.D. “Boundary elements approach for solving stochastic nonlinear problems with fractional laplacian terms” Probabilistic Engineering Mechanics, **59**, art. 103031 (2020).
13. Spanos, P.D., Malara, G. “Nonlinear vibrations of beams and plates with fractional derivative elements subjected to combined harmonic and random excitations”, Probabilistic Engineering Mechanics, **59**, art. 103043 (2020).
14. Zhang, Y., Spanos, P.D. “A linearization scheme for vibrations due to combined deterministic and stochastic loads”, Probabilistic Engineering Mechanics, **60**, art. 103028 (2020).
15. Liu, L., Xu, W., Yue., X., Jia, W. “Stochastic analysis of strongly non-linear elastic impact system with coulomb friction excited by white noise”, Probabilistic Engineering Mechanics, **61**, art. 103085 (2020).
16. Podworna, M., Sniady, P., Grosel, J. “Random vibrations of a structure modified by damped absorbers”, Probabilistic Engineering Mechanics, **66**, art. 103151 (2021).
17. Jablonka, A., Iwankiewicz, R. “Dynamic response of a beam to the train of moving forces driven by an Erlang renewal process”, Probabilistic Engineering Mechanics, **66**, art. 103155 (2021).
18. Golecki, T., Gomez, F., Carrion, J., Spencer, Jr, B.F. “Continuous random field representation of stochastic moving loads”, Probabilistic Engineering Mechanics, **68**, art. 103230 (2022).
19. Rofooei, F.R., Nikkhoo, A. “Application of active piezoelectric patches in controlling the dynamic response of a thin rectangular plate under a moving mass”, International Journal of Solids and Structures **46**, pp. 2429 – 2443 (2009).
20. Nikkhoo, A., Rofooei, F.R. “Parametric study of the dynamic response of thin rectangular plates traversed by moving mass”, Acta Mechanica **223**, pp. 15 – 27 (2012).
21. Nikkhoo, A., Hassanabadi, M.E., Azam, S.E., Amiri, J.V. “Vibration of a thin rectangular plate subjected to series of moving inertial loads”, Mechanics Research Communications **55**, pp.105 – 113 (2014).
22. Ghazvini, T., Nikkhoo, A., Allahyari, H., Zalpuli, M. “Dynamic response analysis of a thin rectangular plate of varying thickness to a traveling inertial load”, Journal of the Brazilian Society of Mechanical Sciences and Engineering **38**, pp. 403 – 411 (2016).
23. Hassanabadi, M.E., Attari, N.K.A., Nikkhoo, A., Mariani, S. “Resonance of a rectangular plate influenced by sequential moving masses”, Coupled Systems Mechanics, **5**(1), pp. 87 – 110 (2016).
24. Rofooei, F.R., Enshaeian, A., Nikkhoo, A. “Dynamic response of geometrically nonlinear, elastic rectangular plates under a moving mass loading by inclusion of all inertial components”, Journal of Sound and Vibration, **394**, pp. 497 – 514 (2017).
25. Nikkhoo, A., Tafakor, R., Mofid, M. “An exact solution to the problems of flexo-poro-elastic structures rested on elastic beds acted upon by moving loads”, Scientia Iranica **27**, pp. 2326 – 2341 (2019).
26. Nikkhoo, A., Banihashemi, Sh., Kiani, K. “Parametric investigations on dynamics of cracked thin rectangular plates excited by a moving mass”, Scientia Iranica (2022) https://doi.org/10.24200/SCI.2022.58345.5686
27. Fryba, L. “Vibration of solids and structures under moving loads”, Thomas Telford, London (1999).
28. Crandal, S.H. “Random vibration of one – and two – dimensional structures”, Developments in Statistics, **2**, pp. 1 – 82 (1978).
29. Leissa, A.W. “Vibration of Plates”, US Government Printing Office, Washington, DC (1969).
30. Bolotin, V.V. “Statistical Methods in Engineering Mechanics”, Stroiizdat, Moscow (1965).

31. Chakraverty, S. “Vibration of plates”, CRC Press, Boca Raton (2010).
32. Bhat, R.B. “Natural frequencies of rectangular plates using characteristic orthogonal polynomials in Rayleigh-Ritz method”, Journal of sound and vibration **102**(4), pp. 493 – 499 (1985).
33. Haung, C.S., Leissa, A.W., Chan, C.W. “Vibrations of rectangular plates with internal cracks or slits”, International Journal of Mechanical Sciences **53**, pp. 436 – 445 (2011).
34. Boresi, A.P., Schmidt, R.J. “Advanced mechanics of materials”, John Wiley & Sons, Inc., New York (2002).
35. Chopra, A.K., “Dynamics of structures theory and applications to earthquake engineering in SI”, Pearson Prentice Hall, Upper Saddle River (2019).
36. Leissa, A.W., “Vibration of Plates”, US Government Printing Office, Washington, DC (1969).

Captions of the figures:

Figure 1. Behavior of the functions of z in time at the middle point of a simply-supported (a) undamped intact rectangular plate (b) damped intact rectangular plate (c) undamped beam (d) damped beam subjected to the moving random load with the white noise covariance.

Figure 2. Behavior of the functions of z in time at the middle point of a simply-supported (a) undamped intact rectangular plate (b) damped intact rectangular plate (c) undamped beam (d) damped beam subjected to the moving random load with the constant covariance.

Figure 3. Behavior of the functions of z in time at the middle point of a simply-supported (a) undamped intact rectangular plate (b) damped intact rectangular plate (c) undamped beam (d) damped beam subjected to the moving random load with the exponential cosine covariance.

Figure 4. Behavior of the functions of z in time at the middle point of a simply-supported (a) undamped cracked rectangular plate compare with undamped intact plate (b) damped cracked rectangular plate compare with damped intact plate subjected to the moving random load with the white noise covariance.

Figure 5. Behavior of the functions of z in time at the middle point of a simply-supported (a) undamped cracked rectangular plate compare with undamped intact plate (b) damped cracked rectangular plate compare with damped intact plate subjected to the moving random load with the constant covariance.

Figure 6. Behavior of the functions of z in time at the middle point of a simply-supported (a) undamped cracked rectangular plate compare with undamped intact plate (b) damped cracked rectangular plate compare with damped intact plate subjected to the moving random load with the exponential cosine covariance.

Figure 7. Behavior of the functions of z in time at the middle point of a simply-supported (a) undamped cracked rectangular plate versus undamped intact plate (b) damped cracked rectangular plate versus damped intact plate subjected to the moving random load with the exponential covariance.

Figure 8. Behavior of the functions of z in time at the middle point of a simply-supported (a) undamped cracked rectangular plate versus undamped intact plate (b) damped cracked rectangular plate versus damped intact plate subjected to the moving random load with the cosine wave covariance pattern.

Figure 9. Behavior of the functions of z in time at the middle point of a simply-supported damped cracked rectangular plate with different crack lengths and different inclined crack angles subjected to the moving random load with the (a) – (b) white noise covariance (c) – (d) constant covariance (e) – (f) exponential cosine covariance.

Figure 10. Effects of inclined crack angles on the functions of z at the middle point of a simply-supported damped cracked rectangular plate with constant crack lengths and different inclined crack angles subjected to the moving random load with the white noise covariance pattern.

Figure 11. Effects of inclined crack angles on the functions of z at the middle point of a simply-supported damped cracked rectangular plate with constant crack lengths and different inclined crack angles subjected to the moving random load with the constant covariance.

Figure 12. Effects of inclined crack angles on the functions of z at the middle point of a simply-supported damped cracked rectangular plate with constant crack lengths and different inclined crack angles subjected to the moving random load with the exponential cosine covariance.

Figure 13. Effects of inclined crack angles on the functions of z at the middle point of a simply-supported damped cracked rectangular plate with constant crack lengths and different inclined crack angles subjected to the moving random load with the exponential covariance.

Figure 14. Effects of inclined crack angles on the functions of z at the middle point of a simply-supported damped cracked rectangular plate with constant crack lengths and different inclined crack angles subjected to the moving random load with the cosine wave covariance.

Figure 15. Effects of crack lengths on the functions of z at the middle point of a simply-supported damped cracked rectangular plate with different crack lengths and constant inclined crack angles subjected to the moving random load with the white noise covariance.

Figure 16. Effects of crack lengths on the functions of z at the middle point of a simply-supported damped cracked rectangular plate with different crack lengths and constant inclined crack angles subjected to the moving random load with the constant covariance.

Figure 17. Effects of crack lengths on the functions of z at the middle point of a simply-supported damped cracked rectangular plate with different crack lengths and constant inclined crack angles subjected to the moving random load with the exponential cosine covariance.

Figure 18. Effects of crack lengths on the functions of z at the middle point of a simply-supported damped cracked rectangular plate with different crack lengths and constant inclined crack angles subjected to the moving random load with the exponential covariance.

Figure 19. Effects of crack lengths on the functions of z at the middle point of a simply-supported damped cracked rectangular plate with different crack lengths and constant inclined crack angles subjected to the moving random load with the cosine wave covariance.

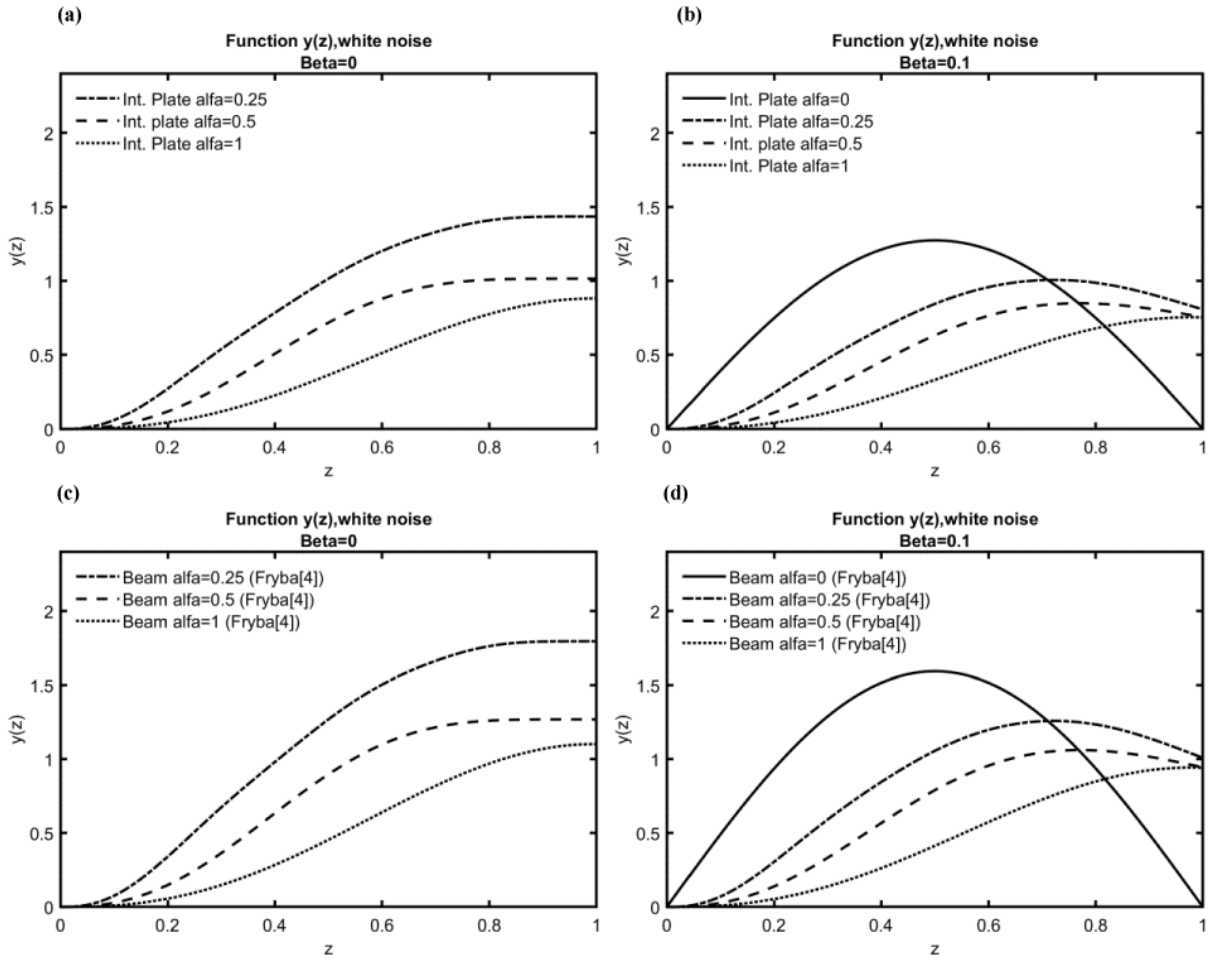
(a)
Function y(z),white noise
Beta=0
Int. Plate alfa=0.25
Int. plate alfa=0.5
Int. Plate alfa=1
y(z)
z
(b)
Function y(z),white noise
Beta=0.1
Int. Plate alfa=0
Int. Plate alfa=0.25
Int. plate alfa=0.5
Int. Plate alfa=1
y(z)
z
(c)
Function y(z),white noise
Beta=0
Beam alfa=0.25 (Fryba[4])
Beam alfa=0.5 (Fryba[4])
Beam alfa=1 (Fryba[4])
y(z)
z
(d)
Function y(z),white noise
Beta=0.1
Beam alfa=0 (Fryba[4])
Beam alfa=0.25 (Fryba[4])
Beam alfa=0.5 (Fryba[4])
Beam alfa=1 (Fryba[4])
y(z)
z

Figure 1.

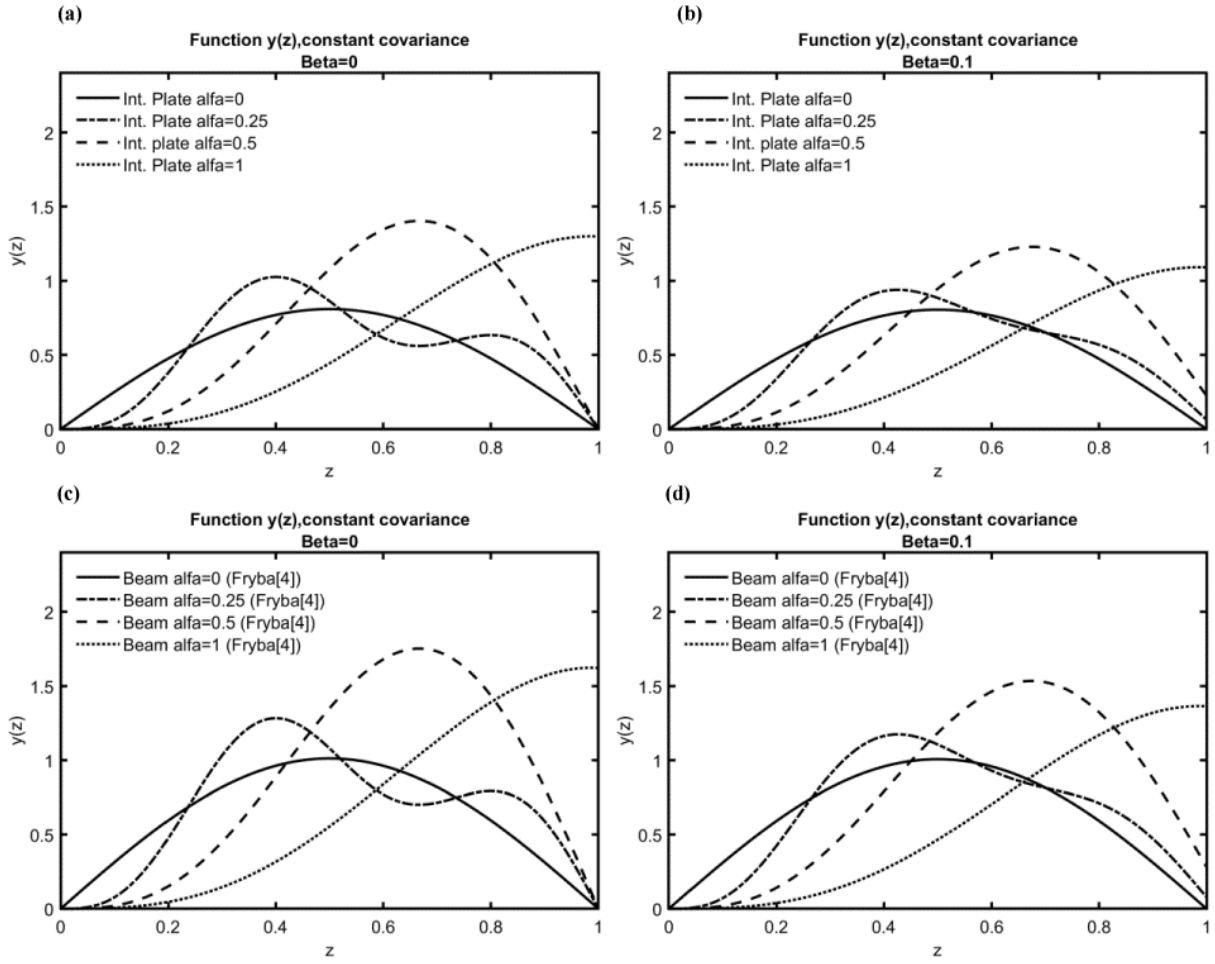
(a)
Function y(z),constant covariance
Beta=0
Int. Plate alfa=0
Int. Plate alfa=0.25
Int. plate alfa=0.5
Int. Plate alfa=1
y(z)
z
(b)
Function y(z),constant covariance
Beta=0.1
Int. Plate alfa=0
Int. Plate alfa=0.25
Int. plate alfa=0.5
Int. Plate alfa=1
y(z)
z
(c)
Function y(z),constant covariance
Beta=0
Beam alfa=0 (Fryba[4])
Beam alfa=0.25 (Fryba[4])
Beam alfa=0.5 (Fryba[4])
Beam alfa=1 (Fryba[4])
y(z)
z
(d)
Function y(z),constant covariance
Beta=0.1
Beam alfa=0 (Fryba[4])
Beam alfa=0.25 (Fryba[4])
Beam alfa=0.5 (Fryba[4])
Beam alfa=1 (Fryba[4])
y(z)
z

Figure 2.

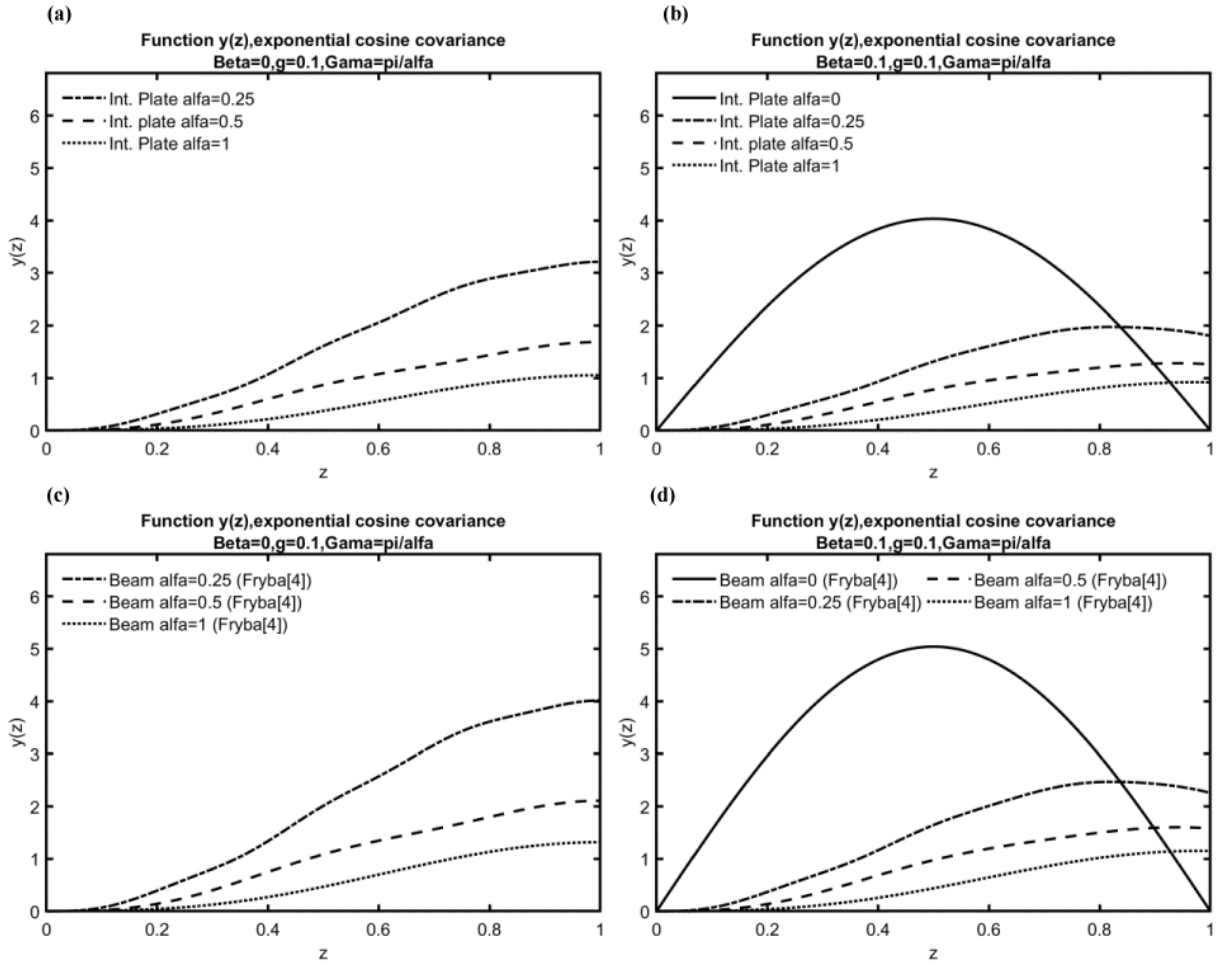
(a)
Function y(z),exponential cosine covariance
Beta=0,g=0.1,Gama=pi/alfa
Int. Plate alfa=0.25
Int. plate alfa=0.5
Int. Plate alfa=1
y(z)
z
(b)
Function y(z),exponential cosine covariance
Beta=0.1,g=0.1,Gama=pi/alfa
Int. Plate alfa=0
Int. Plate alfa=0.25
Int. plate alfa=0.5
Int. Plate alfa=1
y(z)
z
(c)
Function y(z),exponential cosine covariance
Beta=0,g=0.1,Gama=pi/alfa
Beam alfa=0.25 (Fryba[4])
Beam alfa=0.5 (Fryba[4])
Beam alfa=1 (Fryba[4])
y(z)
z
(d)
Function y(z),exponential cosine covariance
Beta=0.1,g=0.1,Gama=pi/alfa
Beam alfa=0 (Fryba[4])
Beam alfa=0.5 (Fryba[4])
Beam alfa=0.25 (Fryba[4])
Beam alfa=1 (Fryba[4])
y(z)
z

Figure 3.

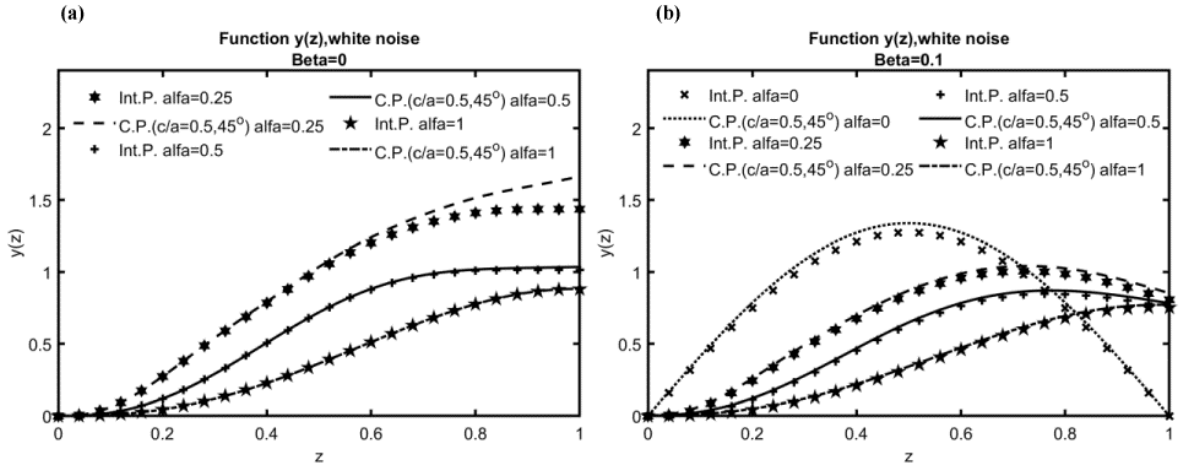

Figure 4.

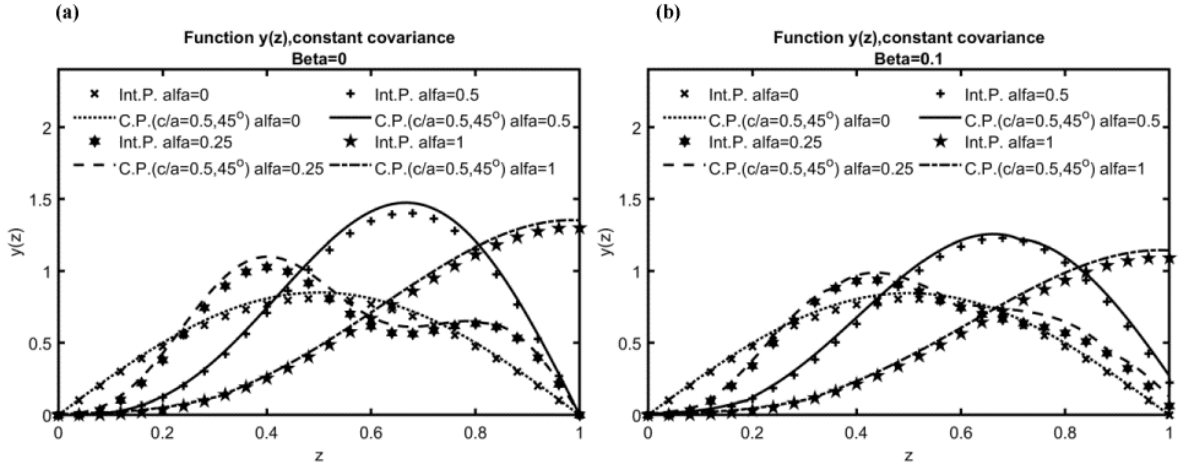

Figure 5.

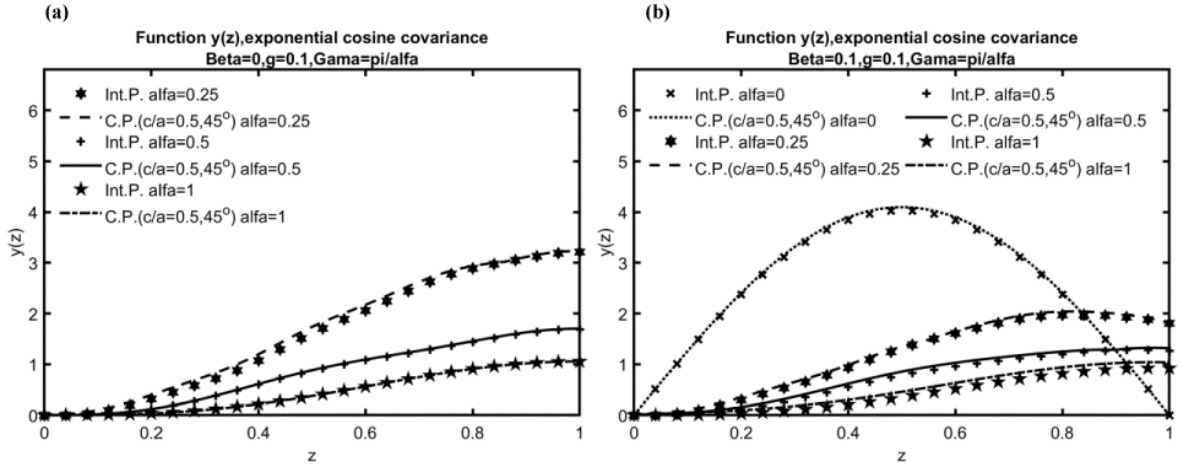

Figure 6.

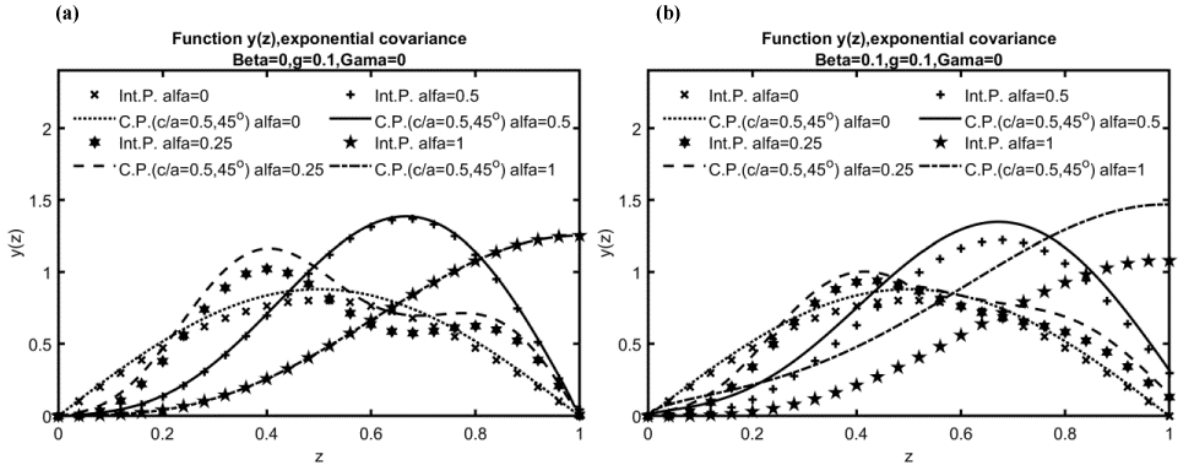

Figure 7.

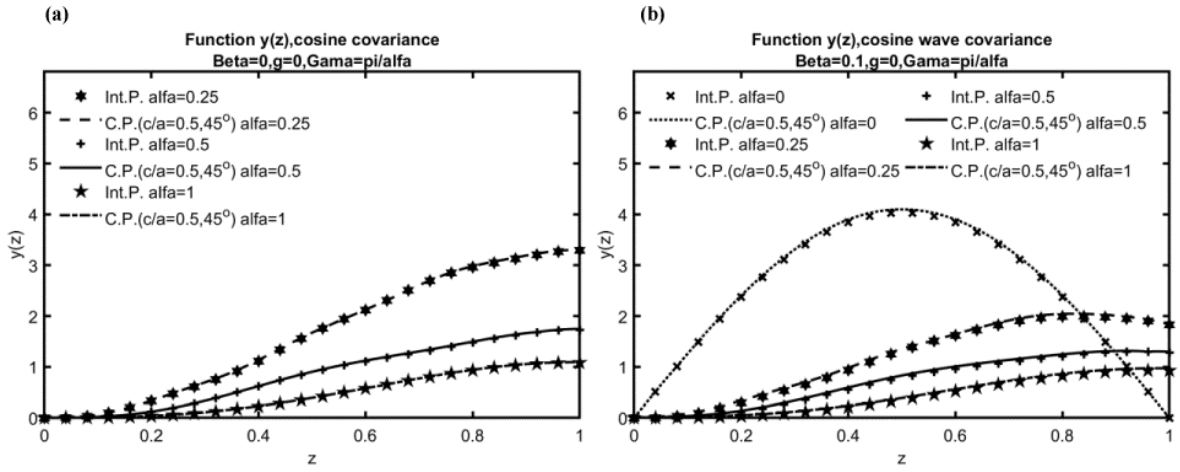

Figure 8.

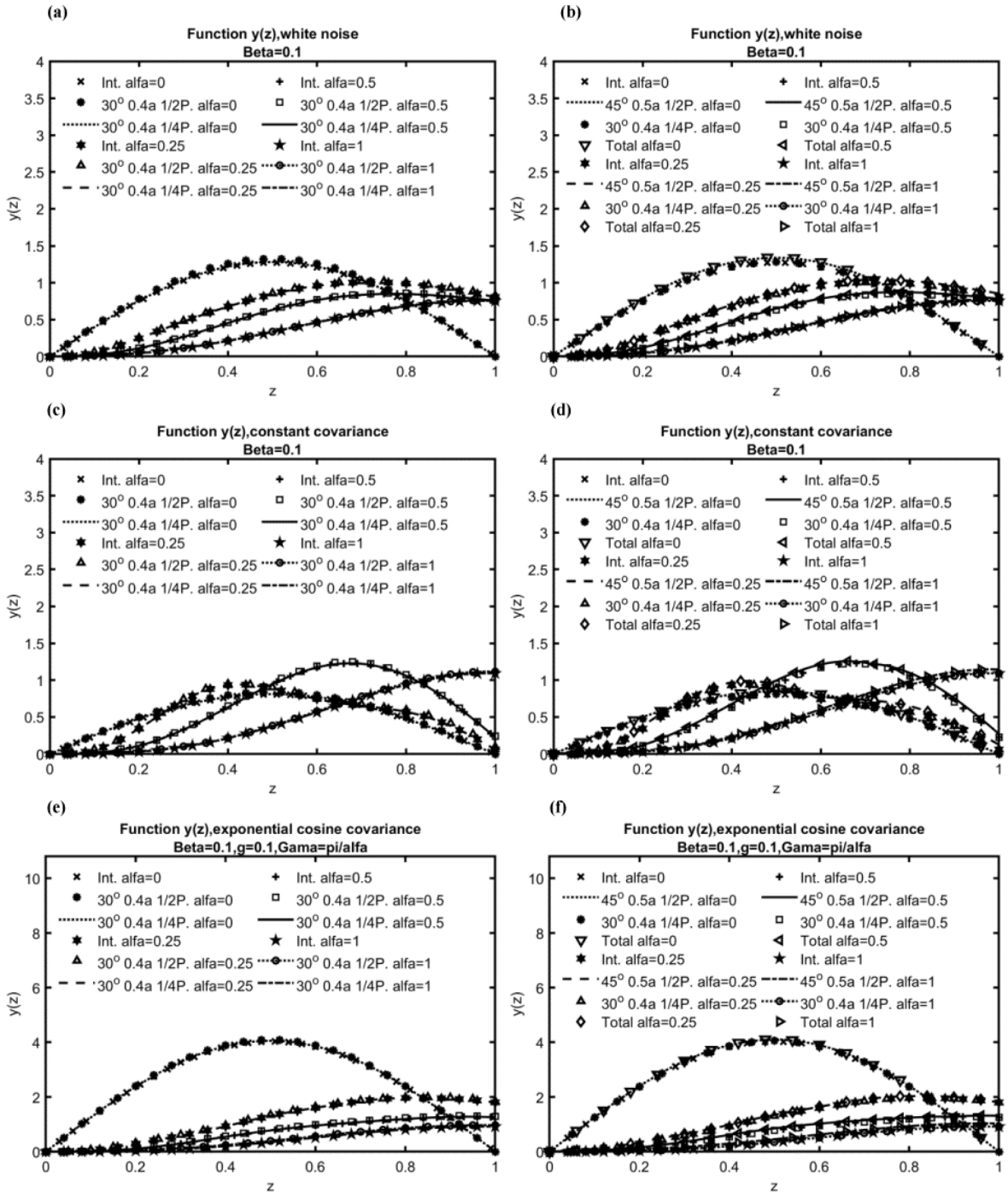
(a)
Function y(z),white noise
Beta=0.1
Int. alfa=0
Int. alfa=0.5
30° 0.4a 1/2P. alfa=0
30° 0.4a 1/2P. alfa=0.5
30° 0.4a 1/4P. alfa=0
30° 0.4a 1/4P. alfa=0.5
Int. alfa=0.25
Int. alfa=1
30° 0.4a 1/2P. alfa=0.25
30° 0.4a 1/2P. alfa=1
30° 0.4a 1/4P. alfa=0.25
30° 0.4a 1/4P. alfa=1
y(z)
z
(b)
Function y(z),white noise
Beta=0.1
Int. alfa=0
Int. alfa=0.5
45° 0.5a 1/2P. alfa=0
45° 0.5a 1/2P. alfa=0.5
30° 0.4a 1/4P. alfa=0
30° 0.4a 1/4P. alfa=0.5
Total alfa=0
Total alfa=0.5
Int. alfa=0.25
Int. alfa=1
45° 0.5a 1/2P. alfa=0.25
45° 0.5a 1/2P. alfa=1
30° 0.4a 1/4P. alfa=0.25
30° 0.4a 1/4P. alfa=1
Total alfa=0.25
Total alfa=1
y(z)
z
(c)
Function y(z),constant covariance
Beta=0.1
Int. alfa=0
Int. alfa=0.5
30° 0.4a 1/2P. alfa=0
30° 0.4a 1/2P. alfa=0.5
30° 0.4a 1/4P. alfa=0
30° 0.4a 1/4P. alfa=0.5
Int. alfa=0.25
Int. alfa=1
30° 0.4a 1/2P. alfa=0.25
30° 0.4a 1/2P. alfa=1
30° 0.4a 1/4P. alfa=0.25
30° 0.4a 1/4P. alfa=1
y(z)
z
(d)
Function y(z),constant covariance
Beta=0.1
Int. alfa=0
Int. alfa=0.5
45° 0.5a 1/2P. alfa=0
45° 0.5a 1/2P. alfa=0.5
30° 0.4a 1/4P. alfa=0
30° 0.4a 1/4P. alfa=0.5
Total alfa=0
Total alfa=0.5
Int. alfa=0.25
Int. alfa=1
45° 0.5a 1/2P. alfa=0.25
45° 0.5a 1/2P. alfa=1
30° 0.4a 1/4P. alfa=0.25
30° 0.4a 1/4P. alfa=1
Total alfa=0.25
Total alfa=1
y(z)
z
(e)
Function y(z),exponential cosine covariance
Beta=0.1,g=0.1,Gama=pi/alfa
Int. alfa=0
Int. alfa=0.5
30° 0.4a 1/2P. alfa=0
30° 0.4a 1/2P. alfa=0.5
30° 0.4a 1/4P. alfa=0
30° 0.4a 1/4P. alfa=0.5
Int. alfa=0.25
Int. alfa=1
30° 0.4a 1/2P. alfa=0.25
30° 0.4a 1/2P. alfa=1
30° 0.4a 1/4P. alfa=0.25
30° 0.4a 1/4P. alfa=1
y(z)
z
(f)
Function y(z),exponential cosine covariance
Beta=0.1,g=0.1,Gama=pi/alfa
Int. alfa=0
Int. alfa=0.5
45° 0.5a 1/2P. alfa=0
45° 0.5a 1/2P. alfa=0.5
30° 0.4a 1/4P. alfa=0
30° 0.4a 1/4P. alfa=0.5
Total alfa=0
Total alfa=0.5
Int. alfa=0.25
Int. alfa=1
45° 0.5a 1/2P. alfa=0.25
45° 0.5a 1/2P. alfa=1
30° 0.4a 1/4P. alfa=0.25
30° 0.4a 1/4P. alfa=1
Total alfa=0.25
Total alfa=1
y(z)
z

Figure 9.

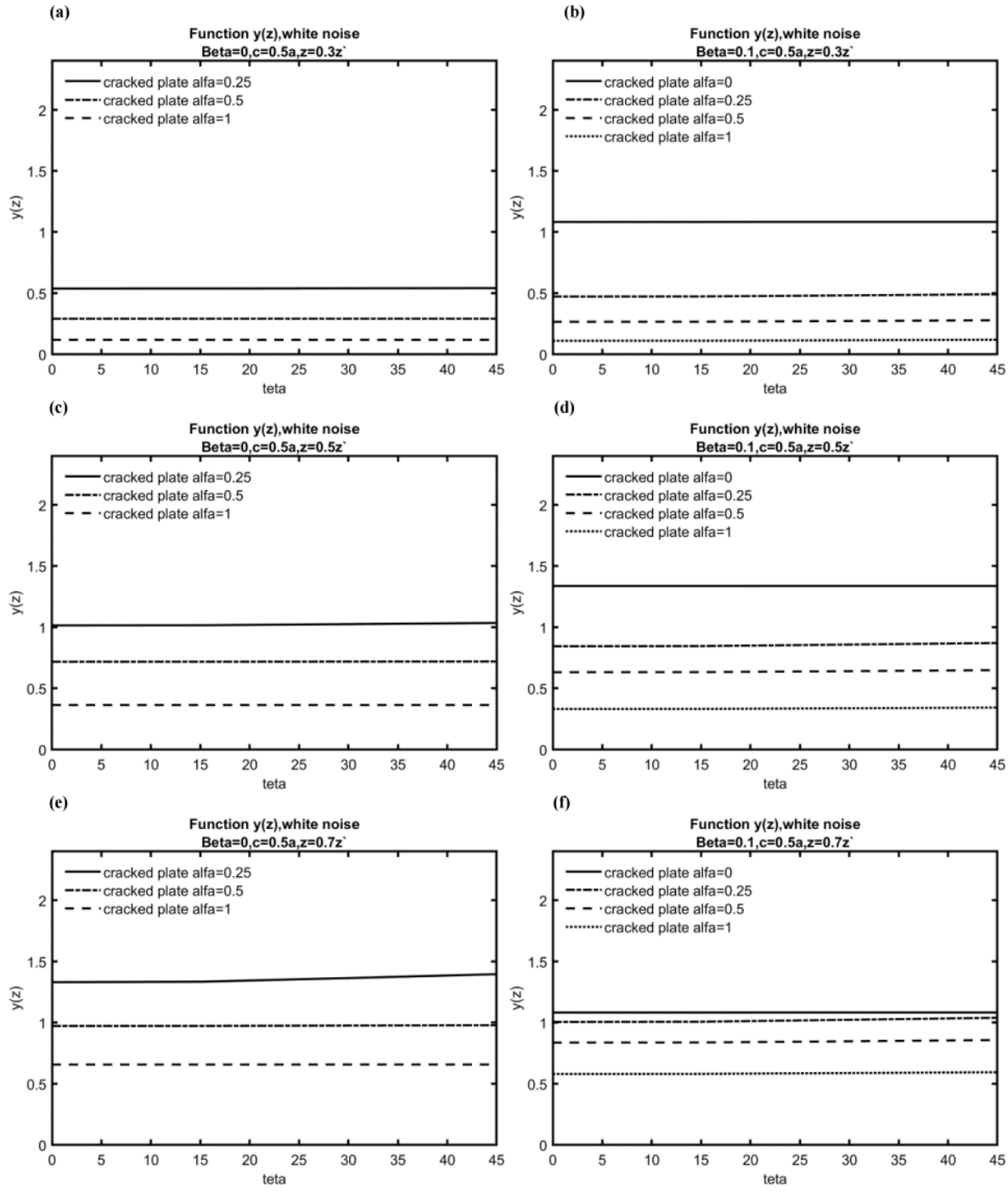
(a)
Function y(z),white noise
Beta=0,c=0.5a,z=0.3z`
cracked plate alfa=0.25
cracked plate alfa=0.5
cracked plate alfa=1
(b)
Function y(z),white noise
Beta=0.1,c=0.5a,z=0.3z`
cracked plate alfa=0
cracked plate alfa=0.25
cracked plate alfa=0.5
cracked plate alfa=1
(c)
Function y(z),white noise
Beta=0,c=0.5a,z=0.5z`
cracked plate alfa=0.25
cracked plate alfa=0.5
cracked plate alfa=1
(d)
Function y(z),white noise
Beta=0.1,c=0.5a,z=0.5z`
cracked plate alfa=0
cracked plate alfa=0.25
cracked plate alfa=0.5
cracked plate alfa=1
(e)
Function y(z),white noise
Beta=0,c=0.5a,z=0.7z`
cracked plate alfa=0.25
cracked plate alfa=0.5
cracked plate alfa=1
(f)
Function y(z),white noise
Beta=0.1,c=0.5a,z=0.7z`
cracked plate alfa=0
cracked plate alfa=0.25
cracked plate alfa=0.5
cracked plate alfa=1
y(z)
teta

Figure 10.

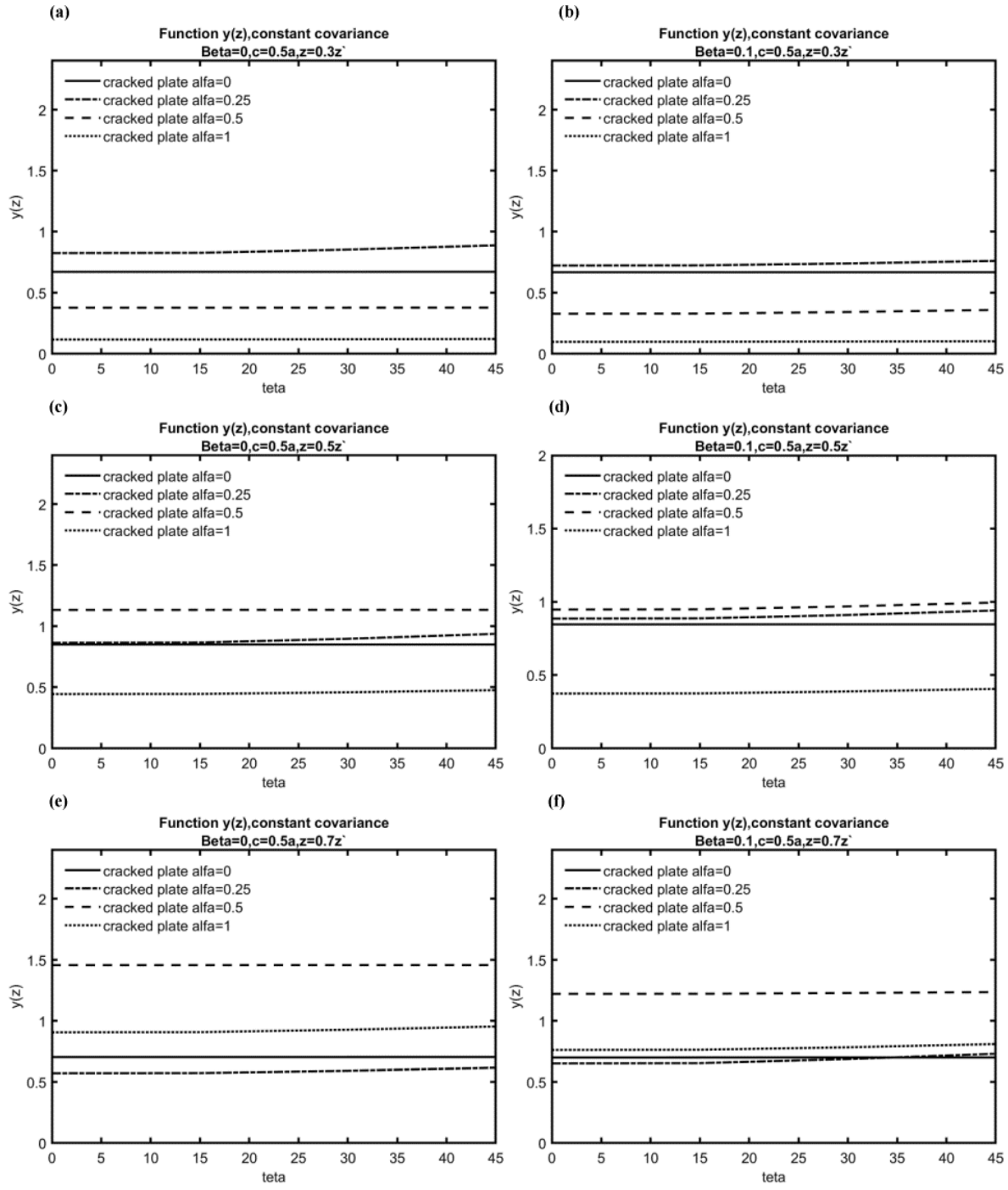
(a)
Function y(z),constant covariance
Beta=0,c=0.5a,z=0.3z`
(b)
Function y(z),constant covariance
Beta=0.1,c=0.5a,z=0.3z`
(c)
Function y(z),constant covariance
Beta=0,c=0.5a,z=0.5z`
(d)
Function y(z),constant covariance
Beta=0.1,c=0.5a,z=0.5z`
(e)
Function y(z),constant covariance
Beta=0,c=0.5a,z=0.7z`
(f)
Function y(z),constant covariance
Beta=0.1,c=0.5a,z=0.7z`
cracked plate alfa=0
cracked plate alfa=0.25
cracked plate alfa=0.5
cracked plate alfa=1
y(z)
teta

Figure 11.

.

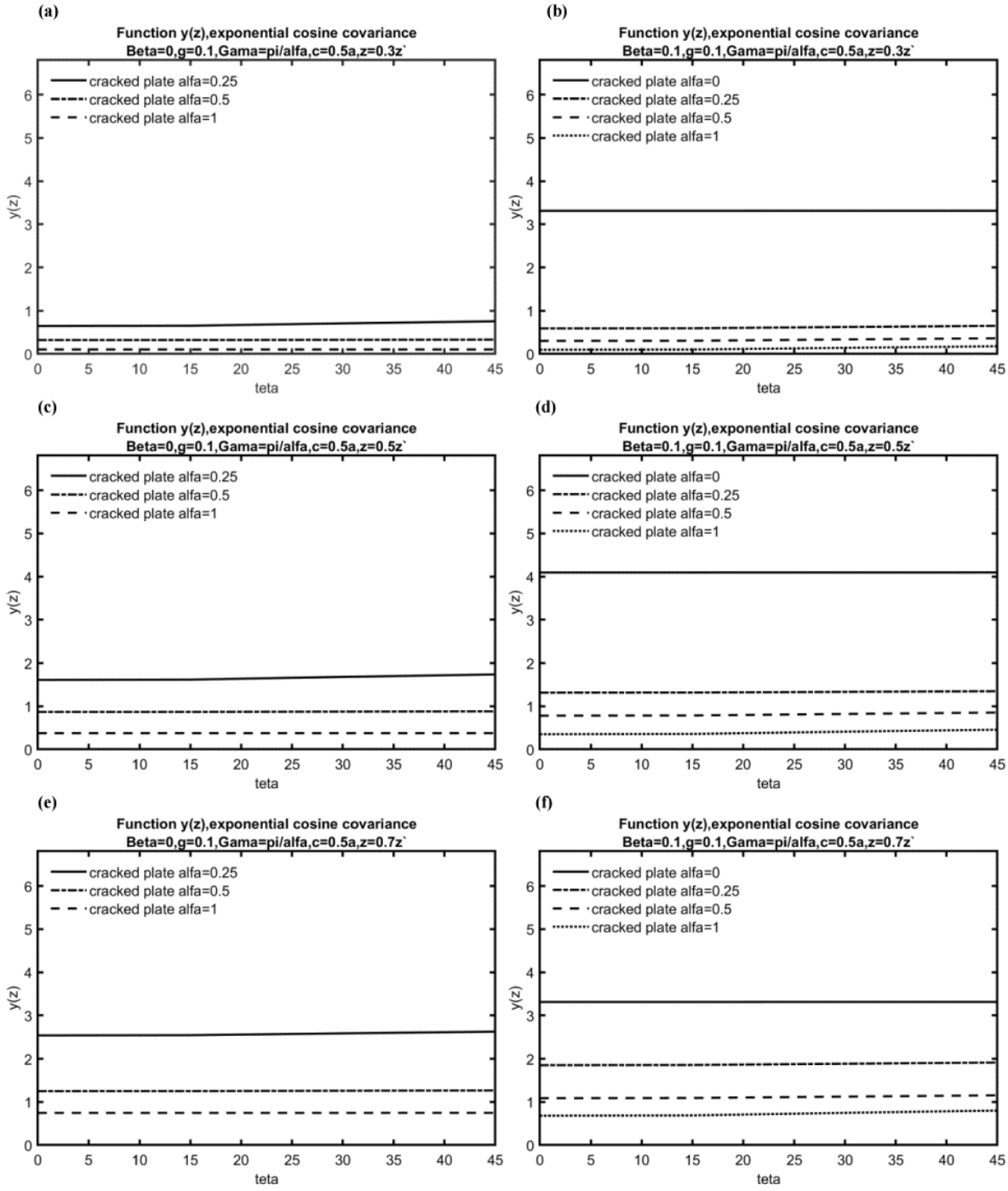
(a)
Function y(z),exponential cosine covariance
Beta=0,g=0.1,Gama=pi/alfa,c=0.5a,z=0.3z`
cracked plate alfa=0.25
cracked plate alfa=0.5
cracked plate alfa=1
y(z)
teta
(b)
Function y(z),exponential cosine covariance
Beta=0.1,g=0.1,Gama=pi/alfa,c=0.5a,z=0.3z`
cracked plate alfa=0
cracked plate alfa=0.25
cracked plate alfa=0.5
cracked plate alfa=1
y(z)
teta
(c)
Function y(z),exponential cosine covariance
Beta=0,g=0.1,Gama=pi/alfa,c=0.5a,z=0.5z`
cracked plate alfa=0.25
cracked plate alfa=0.5
cracked plate alfa=1
y(z)
teta
(d)
Function y(z),exponential cosine covariance
Beta=0.1,g=0.1,Gama=pi/alfa,c=0.5a,z=0.5z`
cracked plate alfa=0
cracked plate alfa=0.25
cracked plate alfa=0.5
cracked plate alfa=1
y(z)
teta
(e)
Function y(z),exponential cosine covariance
Beta=0,g=0.1,Gama=pi/alfa,c=0.5a,z=0.7z`
cracked plate alfa=0.25
cracked plate alfa=0.5
cracked plate alfa=1
y(z)
teta
(f)
Function y(z),exponential cosine covariance
Beta=0.1,g=0.1,Gama=pi/alfa,c=0.5a,z=0.7z`
cracked plate alfa=0
cracked plate alfa=0.25
cracked plate alfa=0.5
cracked plate alfa=1
y(z)
teta

Figure 12.

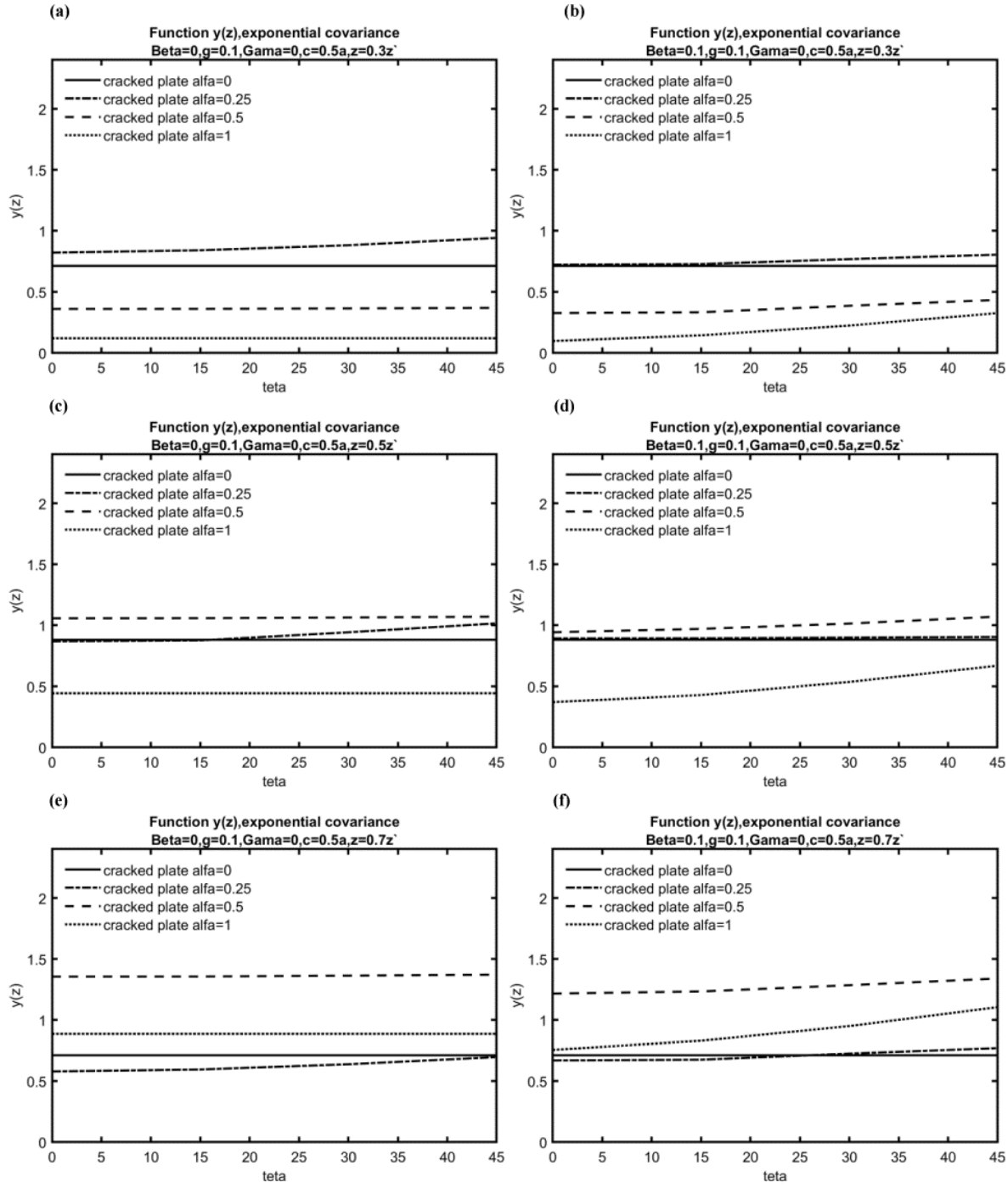
(a)
Function y(z),exponential covariance
Beta=0,g=0.1,Gama=0,c=0.5a,z=0.3z`
(b)
Function y(z),exponential covariance
Beta=0.1,g=0.1,Gama=0,c=0.5a,z=0.3z`
(c)
Function y(z),exponential covariance
Beta=0,g=0.1,Gama=0,c=0.5a,z=0.5z`
(d)
Function y(z),exponential covariance
Beta=0.1,g=0.1,Gama=0,c=0.5a,z=0.5z`
(e)
Function y(z),exponential covariance
Beta=0,g=0.1,Gama=0,c=0.5a,z=0.7z`
(f)
Function y(z),exponential covariance
Beta=0.1,g=0.1,Gama=0,c=0.5a,z=0.7z`
cracked plate alfa=0
cracked plate alfa=0.25
cracked plate alfa=0.5
cracked plate alfa=1
y(z)
teta

Figure 13.

.

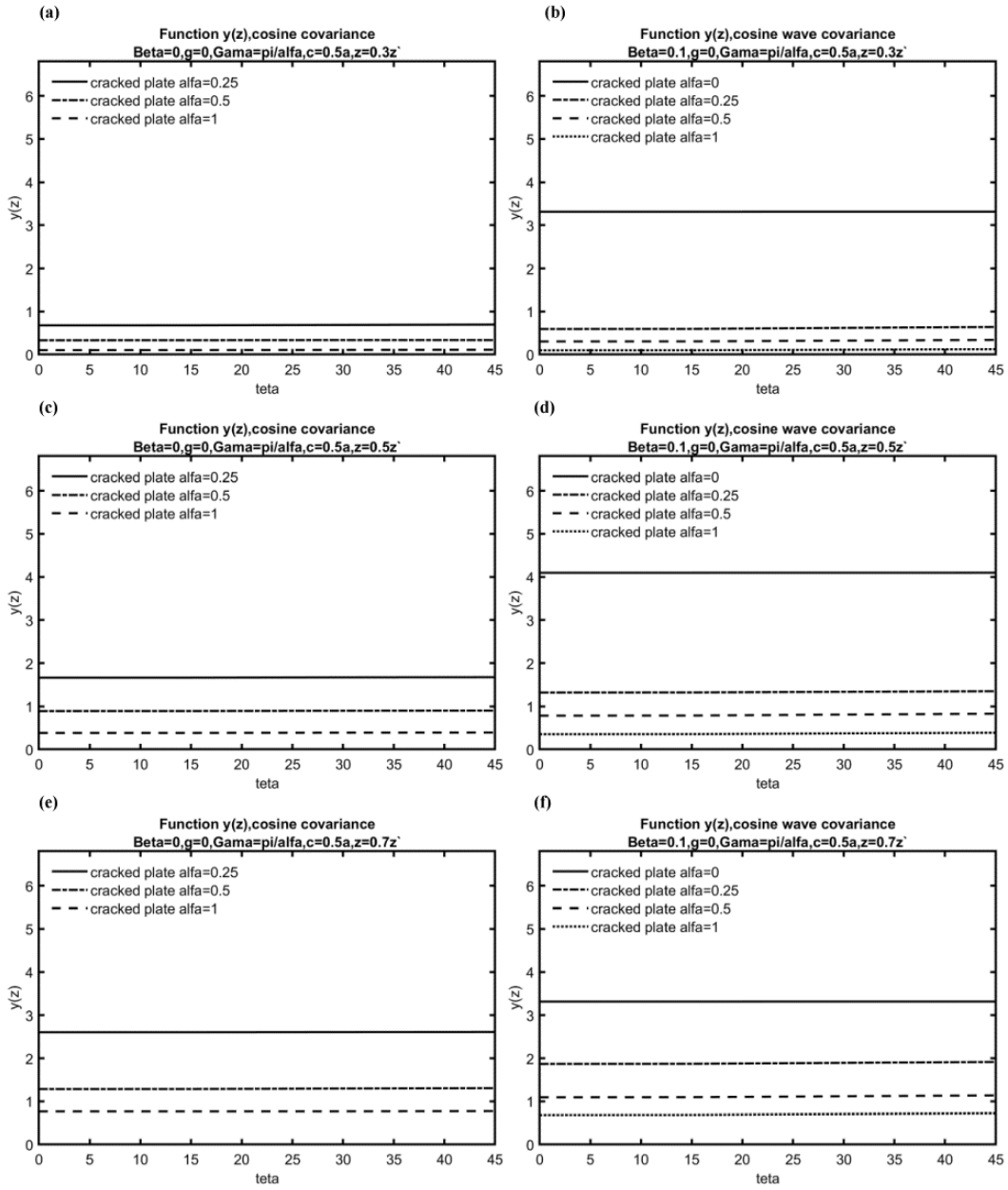
(a)
Function y(z),cosine covariance
Beta=0,g=0,Gama=pi/alfa,c=0.5a,z=0.3z`
cracked plate alfa=0.25
cracked plate alfa=0.5
cracked plate alfa=1
y(z)
teta
(b)
Function y(z),cosine wave covariance
Beta=0.1,g=0,Gama=pi/alfa,c=0.5a,z=0.3z`
cracked plate alfa=0
cracked plate alfa=0.25
cracked plate alfa=0.5
cracked plate alfa=1
y(z)
teta
(c)
Function y(z),cosine covariance
Beta=0,g=0,Gama=pi/alfa,c=0.5a,z=0.5z`
cracked plate alfa=0.25
cracked plate alfa=0.5
cracked plate alfa=1
y(z)
teta
(d)
Function y(z),cosine wave covariance
Beta=0.1,g=0,Gama=pi/alfa,c=0.5a,z=0.5z`
cracked plate alfa=0
cracked plate alfa=0.25
cracked plate alfa=0.5
cracked plate alfa=1
y(z)
teta
(e)
Function y(z),cosine covariance
Beta=0,g=0,Gama=pi/alfa,c=0.5a,z=0.7z`
cracked plate alfa=0.25
cracked plate alfa=0.5
cracked plate alfa=1
y(z)
teta
(f)
Function y(z),cosine wave covariance
Beta=0.1,g=0,Gama=pi/alfa,c=0.5a,z=0.7z`
cracked plate alfa=0
cracked plate alfa=0.25
cracked plate alfa=0.5
cracked plate alfa=1
y(z)
teta

Figure 14.

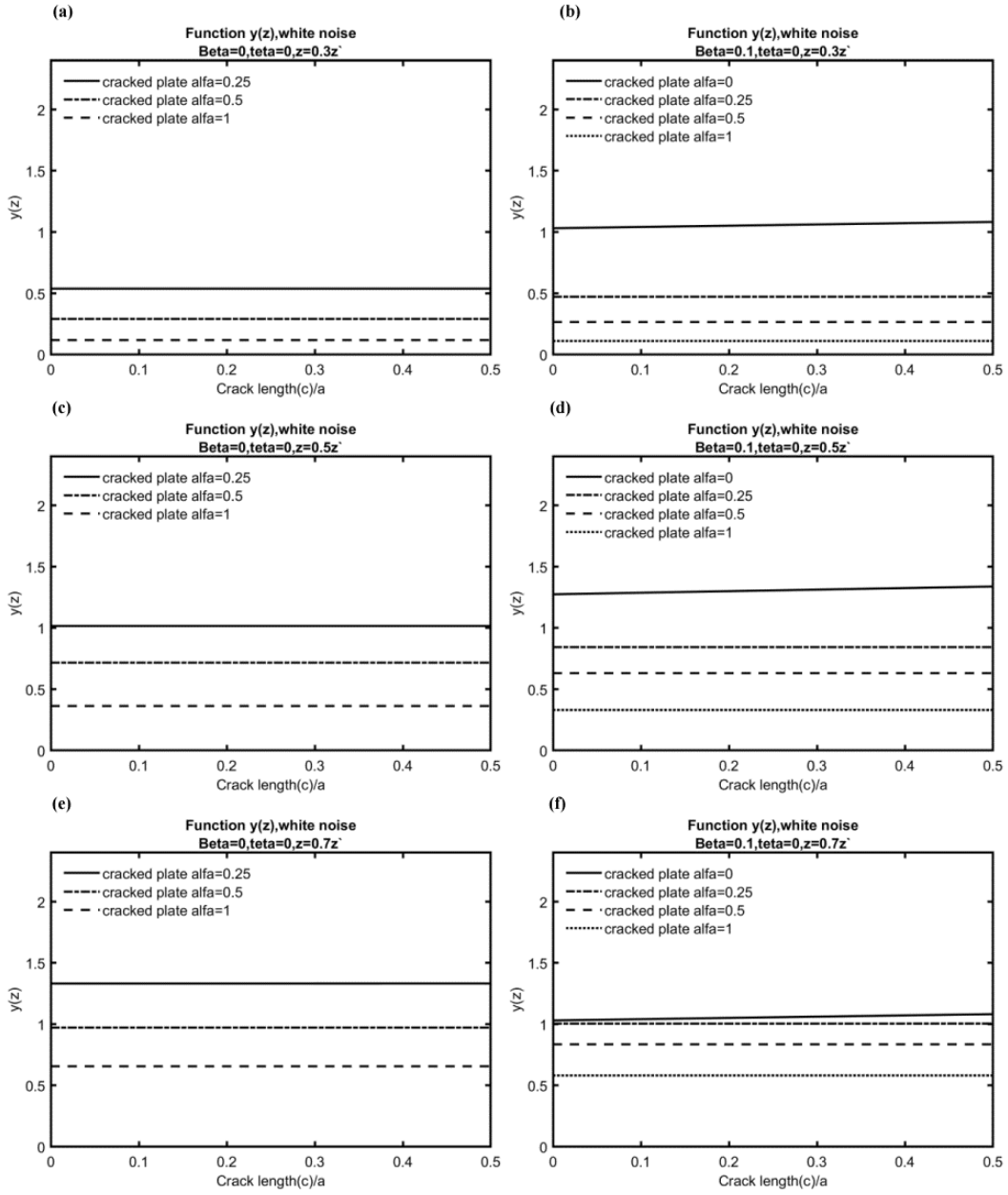
(a)
Function y(z),white noise
Beta=0,teta=0,z=0.3z`
cracked plate alfa=0.25
cracked plate alfa=0.5
cracked plate alfa=1
y(z)
Crack length(c)/a
(b)
Function y(z),white noise
Beta=0.1,teta=0,z=0.3z`
cracked plate alfa=0
cracked plate alfa=0.25
cracked plate alfa=0.5
cracked plate alfa=1
y(z)
Crack length(c)/a
(c)
Function y(z),white noise
Beta=0,teta=0,z=0.5z`
cracked plate alfa=0.25
cracked plate alfa=0.5
cracked plate alfa=1
y(z)
Crack length(c)/a
(d)
Function y(z),white noise
Beta=0.1,teta=0,z=0.5z`
cracked plate alfa=0
cracked plate alfa=0.25
cracked plate alfa=0.5
cracked plate alfa=1
y(z)
Crack length(c)/a
(e)
Function y(z),white noise
Beta=0,teta=0,z=0.7z`
cracked plate alfa=0.25
cracked plate alfa=0.5
cracked plate alfa=1
y(z)
Crack length(c)/a
(f)
Function y(z),white noise
Beta=0.1,teta=0,z=0.7z`
cracked plate alfa=0
cracked plate alfa=0.25
cracked plate alfa=0.5
cracked plate alfa=1
y(z)
Crack length(c)/a

Figure 15.

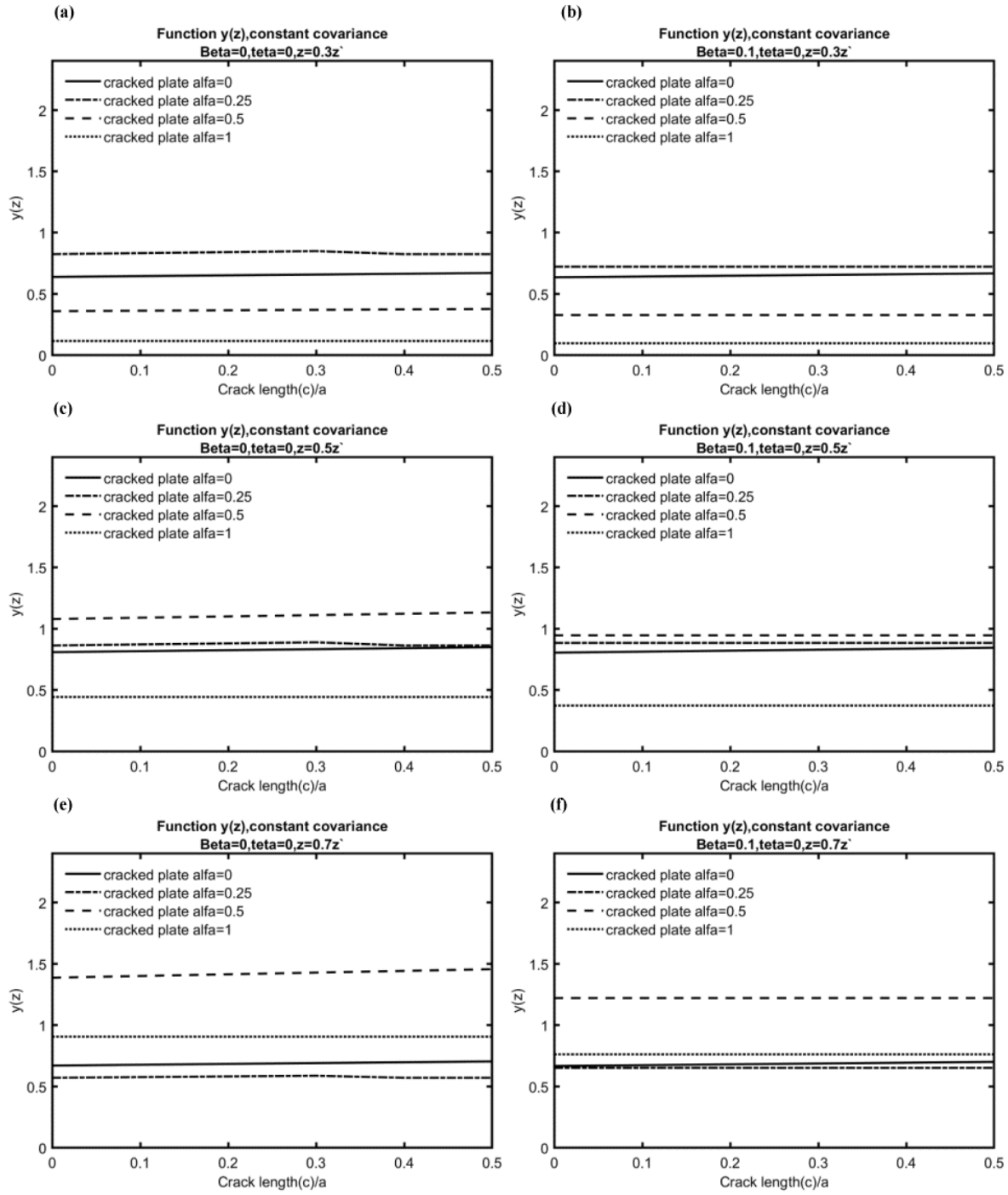
(a)
Function y(z),constant covariance
Beta=0,teta=0,z=0.3z`
(b)
Function y(z),constant covariance
Beta=0.1,teta=0,z=0.3z`
(c)
Function y(z),constant covariance
Beta=0,teta=0,z=0.5z`
(d)
Function y(z),constant covariance
Beta=0.1,teta=0,z=0.5z`
(e)
Function y(z),constant covariance
Beta=0,teta=0,z=0.7z`
(f)
Function y(z),constant covariance
Beta=0.1,teta=0,z=0.7z`
cracked plate alfa=0
cracked plate alfa=0.25
cracked plate alfa=0.5
cracked plate alfa=1
y(z)
Crack length(c)/a

Figure 16.

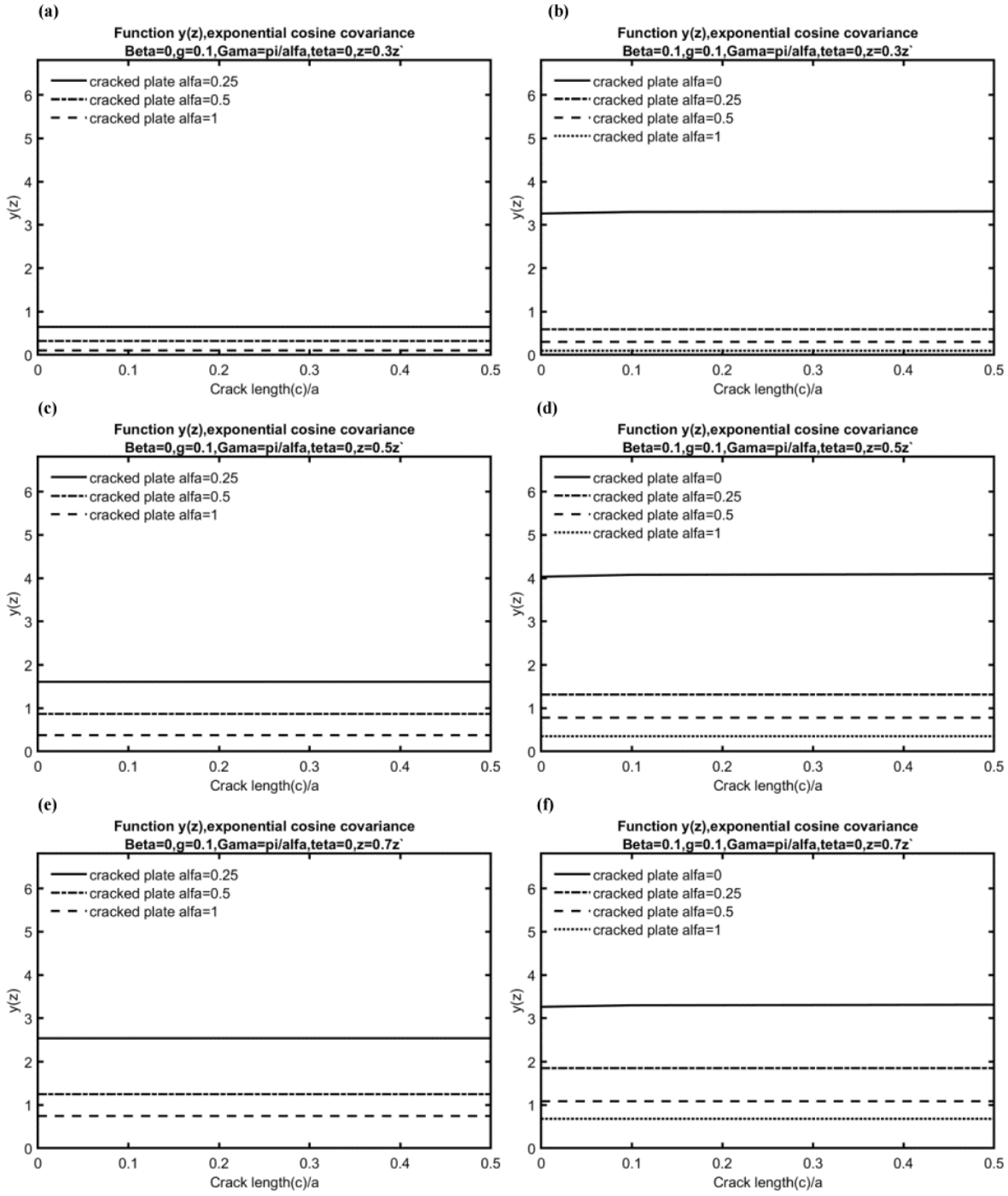
(a)
Function y(z),exponential cosine covariance
Beta=0,g=0.1,Gama=pi/alfa,teta=0,z=0.3z`
cracked plate alfa=0.25
cracked plate alfa=0.5
cracked plate alfa=1
y(z)
Crack length(c)/a
(b)
Function y(z),exponential cosine covariance
Beta=0.1,g=0.1,Gama=pi/alfa,teta=0,z=0.3z`
cracked plate alfa=0
cracked plate alfa=0.25
cracked plate alfa=0.5
cracked plate alfa=1
y(z)
Crack length(c)/a
(c)
Function y(z),exponential cosine covariance
Beta=0,g=0.1,Gama=pi/alfa,teta=0,z=0.5z`
cracked plate alfa=0.25
cracked plate alfa=0.5
cracked plate alfa=1
y(z)
Crack length(c)/a
(d)
Function y(z),exponential cosine covariance
Beta=0.1,g=0.1,Gama=pi/alfa,teta=0,z=0.5z`
cracked plate alfa=0
cracked plate alfa=0.25
cracked plate alfa=0.5
cracked plate alfa=1
y(z)
Crack length(c)/a
(e)
Function y(z),exponential cosine covariance
Beta=0,g=0.1,Gama=pi/alfa,teta=0,z=0.7z`
cracked plate alfa=0.25
cracked plate alfa=0.5
cracked plate alfa=1
y(z)
Crack length(c)/a
(f)
Function y(z),exponential cosine covariance
Beta=0.1,g=0.1,Gama=pi/alfa,teta=0,z=0.7z`
cracked plate alfa=0
cracked plate alfa=0.25
cracked plate alfa=0.5
cracked plate alfa=1
y(z)
Crack length(c)/a

Figure 17.

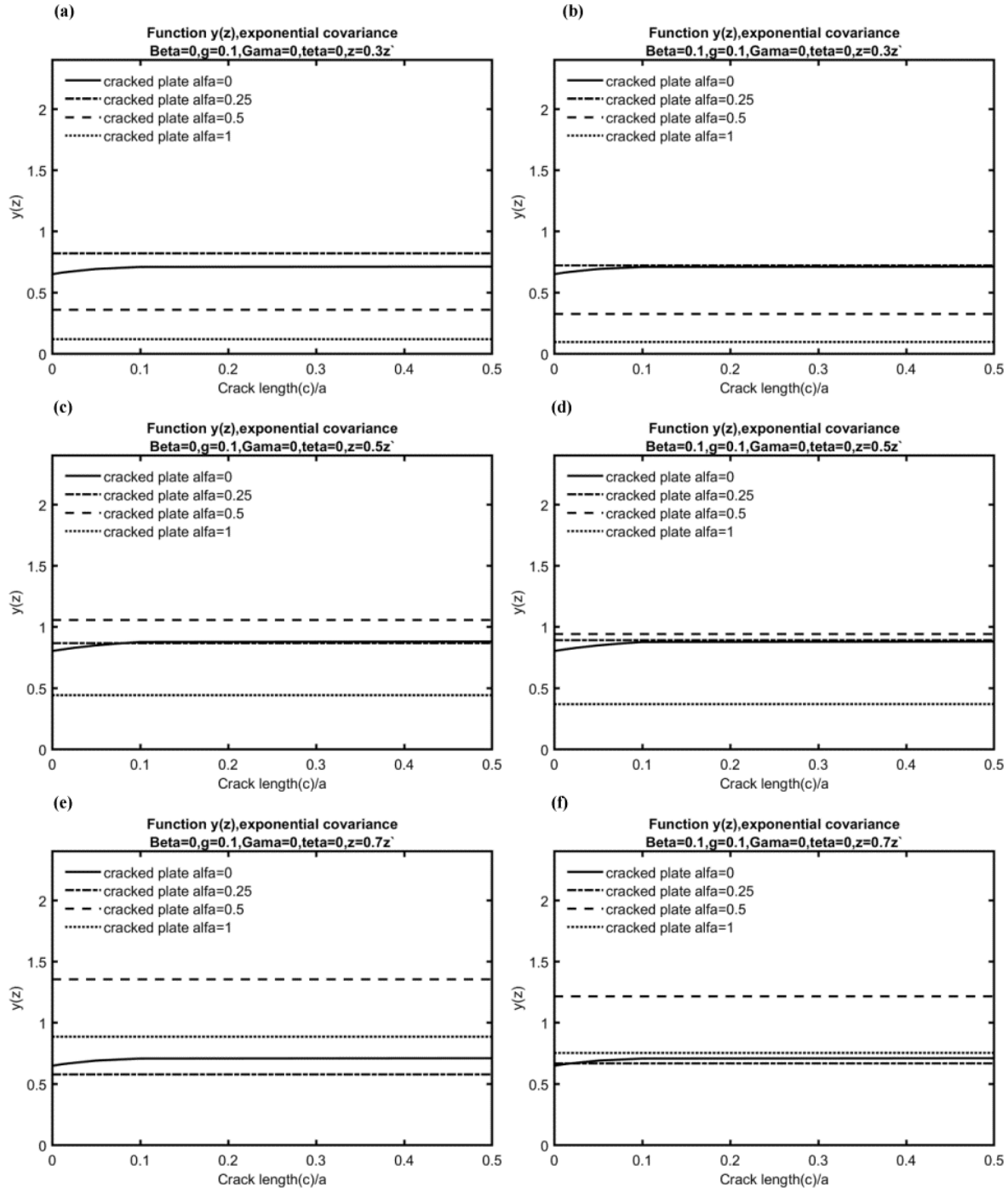
(a)
Function y(z),exponential covariance
Beta=0,g=0.1,Gama=0,teta=0,z=0.3z`
(b)
Function y(z),exponential covariance
Beta=0.1,g=0.1,Gama=0,teta=0,z=0.3z`
(c)
Function y(z),exponential covariance
Beta=0,g=0.1,Gama=0,teta=0,z=0.5z`
(d)
Function y(z),exponential covariance
Beta=0.1,g=0.1,Gama=0,teta=0,z=0.5z`
(e)
Function y(z),exponential covariance
Beta=0,g=0.1,Gama=0,teta=0,z=0.7z`
(f)
Function y(z),exponential covariance
Beta=0.1,g=0.1,Gama=0,teta=0,z=0.7z`
cracked plate alfa=0
cracked plate alfa=0.25
cracked plate alfa=0.5
cracked plate alfa=1
y(z)
Crack length(c)/a

Figure 18.

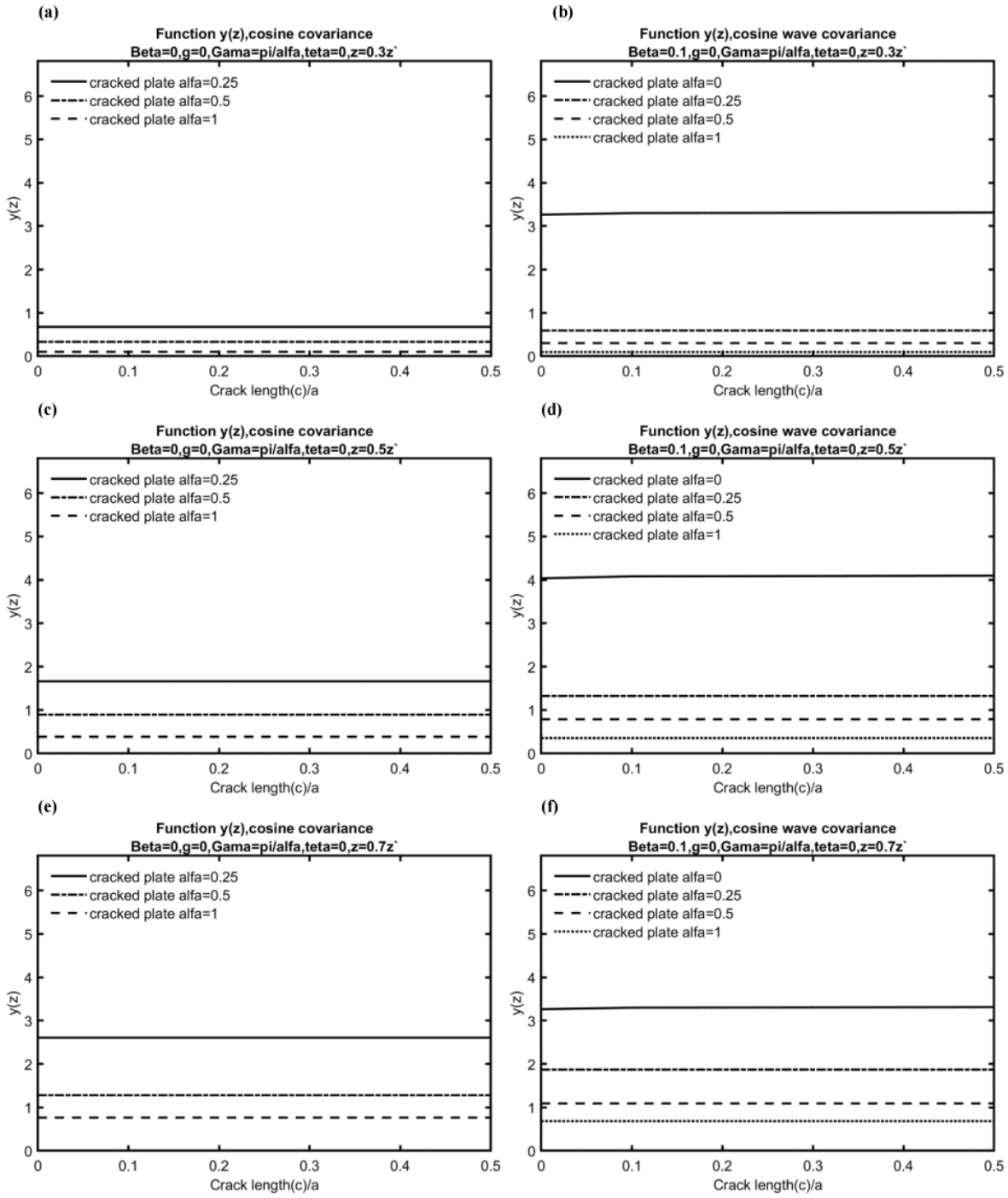
(a)
Function y(z),cosine covariance
Beta=0,g=0,Gama=pi/alfa,teta=0,z=0.3z`
cracked plate alfa=0.25
cracked plate alfa=0.5
cracked plate alfa=1
y(z)
Crack length(c)/a
(b)
Function y(z),cosine wave covariance
Beta=0.1,g=0,Gama=pi/alfa,teta=0,z=0.3z`
cracked plate alfa=0
cracked plate alfa=0.25
cracked plate alfa=0.5
cracked plate alfa=1
y(z)
Crack length(c)/a
(c)
Function y(z),cosine covariance
Beta=0,g=0,Gama=pi/alfa,teta=0,z=0.5z`
cracked plate alfa=0.25
cracked plate alfa=0.5
cracked plate alfa=1
y(z)
Crack length(c)/a
(d)
Function y(z),cosine wave covariance
Beta=0.1,g=0,Gama=pi/alfa,teta=0,z=0.5z`
cracked plate alfa=0
cracked plate alfa=0.25
cracked plate alfa=0.5
cracked plate alfa=1
y(z)
Crack length(c)/a
(e)
Function y(z),cosine covariance
Beta=0,g=0,Gama=pi/alfa,teta=0,z=0.7z`
cracked plate alfa=0.25
cracked plate alfa=0.5
cracked plate alfa=1
y(z)
Crack length(c)/a
(f)
Function y(z),cosine wave covariance
Beta=0.1,g=0,Gama=pi/alfa,teta=0,z=0.7z`
cracked plate alfa=0
cracked plate alfa=0.25
cracked plate alfa=0.5
cracked plate alfa=1
y(z)
Crack length(c)/a

Figure 19.

Biographies

Ali Nikkhoo was born in Tehran of Iran on 1978. He got a B.Sc. degree in civil engineering from Isfahan University of Technology on 2000. Subsequently, he was awarded M.Sc. and Ph.D. degrees with major in structural engineering as an honored student on 2002 and 2008, respectively. His current research is focused on dynamic behavior of beam and plate type structures under the action of moving forces as well as its active control and damage identification in such structural systems. To date, he has published more than 50 articles in peer-reviewed journals of mechanics and mathematics, and has been the reviewer of more than 20 ISI journals.

Keivan Kiani
Dr. Keivan Kiani got B.Sc. degree in civil engineering from Isfahan University of Technology on 2000. Subsequently, he was awarded M.Sc., and Ph.D. degrees with major in structural engineering from Sharif University of Technology in 2002 and 2010, respectively. The expert field of Dr. Kiani is modeling of structures range from nano- to macro- scales. His current research is focus on the wave propagation in, vibrations and dynamic instability of nanostructures using advanced elasticity theories. To date, he has published more than 110 ISI papers in a diverse range of journals of engineering, applied mathematics, and applied physics.

Shirin Banihashemi, received a B.Sc. degree in civil engineering from Khajeh Nasir al Din Toosi University of Technology (KNTU) in Tehran and after studied foundations of civil engineering, studied the acoustics in constructions, included building acoustics and noise controls, room acoustics, technical acoustics, psychoacoustics, electro acoustics, signal analyses and theoretical acoustics, dealt with waves vibrations, as well as dynamics of molecules, named as Brownian movement, at the Graz University of Technology in Austria. According to the relation between acoustical vibrations and structural vibrations, she continued her investigations at the University of Science and Culture (USC) in Tehran, awarding M.Sc. and Ph.D. degrees in structural engineering. Her research interests are focused on acoustical vibrations as well as beam and plate form structures subjected to moving forces as well as moving random forces.